

AD737125



.....contributing to man's  
understanding of the environment world

# A COMPARATIVE STUDY OF THE ELASTIC WAVE RADIATION FROM EARTHQUAKES AND UNDERGROUND EXPLOSIONS

**D.B. LAMBERT  
E.A. FLINN  
SEISMIC DATA LABORATORY**

**C.B. ARCHAMBEAU  
CONSULTANT to the SDL**

**27 OCTOBER 1971**

Prepared for  
**AIR FORCE TECHNICAL APPLICATIONS CENTER**  
Washington, D.C.

Reproduced by  
**NATIONAL TECHNICAL  
INFORMATION SERVICE**  
Springfield, Va. 22151

Under  
**Project VELA UNIFORM**

Sponsored by  
**ADVANCED RESEARCH PROJECTS AGENCY**  
Nuclear Monitoring Research Office  
ARPA Order No. 1714

**DDC**  
**RECEIVED**  
JAN 31 1972  
**REGISTRY**  
**B**

**TELEDYNE GEOTECH**  
ALEXANDRIA LABORATORIES

APPROVED FOR PUBLIC RELEASE; DISTRIBUTION UNLIMITED.

R  
R-163

90

# DISCLAIMER NOTICE

THIS DOCUMENT IS THE BEST  
QUALITY AVAILABLE.

COPY FURNISHED CONTAINED  
A SIGNIFICANT NUMBER OF  
PAGES WHICH DO NOT  
REPRODUCE LEGIBLY.

**DOCUMENT CONTROL DATA - R&D**

(Security classification of title, body of abstract and indexing annotation must be entered when the overall report is classified)

<b>1 ORIGINATING ACTIVITY (Corporate author)</b> Teledyne Geotech Alexandria, Virginia		<b>2a REPORT SECURITY CLASSIFICATION</b> Unclassified	
		<b>2b GROUP</b>	
<b>3 REPORT TITLE</b> A COMPARATIVE STUDY OF THE ELASTIC WAVE RADIATION FROM EARTHQUAKES AND UNDERGROUND EXPLOSIONS			
<b>4 DESCRIPTIVE NOTES (Type of report and inclusive dates)</b> Scientific			
<b>5 AUTHOR(S) (Last name, first name, initial)</b> Lambert, D.G.; Flinn, E.A. and Archambeau, C.B.			
<b>6 REPORT DATE</b> 27 OCTOBER 1971		<b>7a TOTAL NO. OF PAGES</b> 100	<b>7b NO. OF REFS</b> 18
<b>8a CONTRACT OR GRANT NO.</b> F33657-72-C-0009		<b>8b. ORIGINATOR'S REPORT NUMBER(S)</b> 284	
<b>a. PROJECT NO.</b> VELA T/2706		<b>8b. OTHER REPORT NO(S) (Any other numbers that may be assigned this report)</b>	
<b>c. ARPA Order No. 1714</b>			
<b>d. ARPA Program Code No. 2F-10</b>			
<b>10 AVAILABILITY/LIMITATION NOTICES</b>  APPROVED FOR PUBLIC RELEASE; DISTRIBUTION UNLIMITED			
<b>11 SUPPLEMENTARY NOTES</b>		<b>12 SPONSORING MILITARY ACTIVITY</b> Advanced Research Projects Agency Nuclear Monitoring Research Office Washington, D.C.	
<b>13 ABSTRACT</b> <p>A detailed analysis of the surface wave radiation from two underground explosions (BILLBY and SHOAL) and an earthquake (near Fallon, Nevada) whose epicenter is only 60 km from SHOAL indicates that: (1) at long periods the surface wave radiation from the earthquake can be explained by a pure quadrupole (double-couple) source, but at higher frequencies the radiation pattern shows asymmetries which suggest effects due to rupture propagation which require higher-order multipole terms in the source equivalent representation; (2) the surface waves from the explosions can be explained by superposed monopole and quadrupole sources, with no indication of higher-order multipole terms, at least in the frequency range comparable to that in which the earthquake signal was recorded; (3) a principal conclusion of the study is that the anomalous radiation from explosions is due to stress relaxation around the shock-generated shatter zone and not due to earthquake triggering.</p> <p>A comparative analysis of SHOAL and FALLON shows that: (1) the ratio of the Love wave amplitude generated by the earthquake to the Love wave amplitude from the explosion is proportional to the period, which implies a larger source dimension for FALLON; (2) the normalized spectral ratio of Love wave amplitude to Rayleigh wave amplitude, considered as a function of period, is near unity for the explosions but larger for the earthquake by a factor of two or three, and increasing with period. These differences might be useful in distinguishing earthquakes from explosions (at least in the magnitude range of the events used in this study, 4.4 and above), as well as for estimating source parameters (such as stress) which are of fundamental geophysical interest.</p>			
<b>14 KEY WORDS</b> Source Mechanisms Radiation Patterns Stress Relaxation			

*Neither the Advanced Research Projects Agency nor the Air Force Technical Applications Center will be responsible for information contained herein which has been supplied by other organizations or contractors, and this document is subject to later revision as may be necessary. The views and conclusions presented are those of the authors and should not be interpreted as necessarily representing the official policies, either expressed or implied, of the Advanced Research Projects Agency, the Air Force Technical Applications Center, or the U S Government.*

A COMPARATIVE STUDY OF THE ELASTIC WAVE RADIATION FROM  
EARTHQUAKES AND UNDERGROUND EXPLOSIONS  
SEISMIC DATA LABORATORY REPORT NO. 284

AFTAC Project No.: VELA T/2706  
Project Title: Seismic Data Laboratory  
ARPA Order No.: 1714  
ARPA Program Code No.: 2F-10  
  
Name of Contractor: TELEDYNE GEOTECH  
  
Contract No.: F33657-72-C-0009  
Date of Contract: 01 July 1971  
Amount of Contract: \$ 1,290,000  
Contract Expiration Date: 30 June 1972  
Project Manager: Royal A. Hartenberger  
(703) 836-7647

P. O. Box 334, Alexandria, Virginia

*APPROVED FOR PUBLIC RELEASE. DISTRIBUTION UNLIMITED*

## ABSTRACT

A detailed analysis of the surface wave radiation from two underground explosions (BILBY and SHOAL) and an earthquake (near Fallon, Nevada) whose epicenter is only 60 km from SHOAL indicates that: (1) at long periods the surface wave radiation from the earthquake can be explained by a pure quadrupole (double-couple) source, but at higher frequencies the radiation pattern shows asymmetries which suggest effects due to rupture propagation which require higher-order multiple terms in the source equivalent representation; (2) the surface waves from the explosions can be explained by superposed monopole and quadrupole sources, with no indication of higher-order multipole terms, at least in the frequency range comparable to that in which the earthquake signal was recorded; (3) a principal conclusion of the study is that the anomalous radiation from explosions is probably due to stress relaxation around the shock-generated shatter zone and not due to earthquake triggering.

A comparative analysis of SHOAL and FALLON shows that: (1) the ratio of the Love wave amplitude generated by the earthquake to the Love wave amplitude from the explosion is proportional to the period, which implies a larger source dimension for FALLON; (2) the normalized spectral ratio of Love wave amplitude

to Rayleigh wave amplitude, considered as a function of period, is near unity for the explosions but larger for the earthquake by a factor of two or three, and increasing with period. These differences might be useful in distinguishing earthquakes from explosions (at least in the magnitude range of the events used in this study, 4.4 and above), as well as for estimating source parameters (such as stress) which are of fundamental geophysical interest.

## TABLE OF CONTENTS

	Page No.
ABSTRACT	
INTRODUCTION	1
SIGNAL ANALYSIS	5
CONCEPTS AND THEORY	8
SURFACE WAVE RADIATION PATTERNS AND DEDUCTION OF THE EQUIVALENT MULTIPOLE SOURCE	22
Spectral comparisons	35
CONCLUSIONS	47
ACKNOWLEDGMENTS	50
REFERENCES	51
APPENDIX	

## LIST OF FIGURES

Figure Title	Figure No.
Distribution of stations used in the analysis of the SHOAL, Fallon and BILBY events.	1
Long-period LRSM seismometer amplitude response curve. The indicated period range 8-40 second is the band within which good signal power was observed for the events studied.	2
Samples of surface wave signals and the associated group velocity dispersion obtained from these signals using narrow band filtering methods.	3
Samples of surface wave spectra from the three events studied. The signal sample and the group velocity for the BILBY Rayleigh spectra are shown in Figure 3. Fourier spectra of the signals are shown on the left and the group spectra obtained by narrow filtering on the right.	4
Fault (or traction) plane geometry. The point (0) is an arbitrary point of observation, while the vector N is in the direction of geographic North.	5
Variation of the Love to Rayleigh (L/R) wave ratio as a function of $\lambda$ , the (double couple) "slip angle", for superposed monopole and quadrupole (double couple) components. The relative excitation of the quadrupole to monopole component is fixed at $F = 0.58$ for all frequencies.	6
Variation of the Love to Rayleigh (L/R) wave ratio as a function of $\delta$ , the (double couple) "dip angle", for superposed monopole and (double couple) quadrupole components. All other source parameters are fixed, as indicated.	7

LIST OF FIGURES (Cont'd.)

Figure Title	Figure No.
Radiation patterns of Love and Rayleigh waves from the underground explosion BILBY at periods of 15 and 20 seconds. The insets show the theoretical pattern shapes obtained as a fit to the observations using a superposed monopole and quadrupole point source with fixed relative excitation of quadrupole to monopole of $F = 0.5$ , with the quadrupole "strike", $\phi = 342^\circ$ . The point source equivalents are the same for both Love and Rayleigh waves. The factor $\epsilon = 0.7$ is the particle orbit ellipticity factor for the Rayleigh waves and is dependent on the structure used in the theoretical calculations.	8
The theoretical Love to Rayleigh (L/R) wave ratio for BILBY, at $T = 15$ seconds, as a function of azimuth using the source parameters of Figure 8. The observed ratios at a number of stations with good signal to noise ratios for both Love and Rayleigh waves are shown at their appropriate azimuths. This also shows the nature of the L/R azimuth variation and that a single equivalent source fits both Love and Rayleigh wave radiation for this event.	9
Radiation patterns of Love and Rayleigh waves from the underground explosion SHOAL at periods of 15 and 20 seconds. The insets show the theoretical patterns obtained as a fit to the observations using a superposed monopole and quadrupole point source with fixed relative excitation of quadrupole to monopole of $F = 0.58$ , with the quadrupole "strike", $\phi = 353^\circ$ . The point source equivalents are the same for both Love and Rayleigh waves.	10

## LIST OF FIGURES (Cont'd.)

Figure Title	Figure No.
The theoretical Love to Rayleigh (L/R) wave ratio for SHOAL, at $T = 15$ seconds, as a function of azimuth using the source parameters of Figure 10. Observations at various azimuths where signal to noise ratios were high are indicated and identified by abbreviated station symbols. This also shows the nature of the L/R azimuth variation (which is nearly identical to that for BILBY) and that a single equivalent source fits both Love and Rayleigh wave radiation for this event.	11
Radiation patterns for Love waves from the Fallon earthquake at periods of 9, 12, 20 and 30 seconds. The inset shows the theoretical pattern shape obtained as a fit using a point quadrupole (double couple) located and oriented as indicated. The orientation of the quadrupole is close to that obtained for SHOAL, indicating that the stress field orientation was similar for both the data and contours for the field at $T = 9$ seconds (a) show asymmetries in the near-source pattern indicating rupture propagation effects or perturbation in the pattern due to strong lateral variations in structure. These diminish with increasing period (b), (c), and (d), except for the point of observation in northern California. This anomaly may be due to the strong structural variation at the Sierra Nevada - Basin and Range boundary.	12
Radiation patterns for Rayleigh waves from the Fallon earthquake at periods of 9, 12, 16 and 20 seconds. The insets show theoretical patterns from the same point quadrupole source used to obtain the theoretical fits to the Love wave radiation patterns in Figure 12. The theoretical patterns for the Rayleigh waves change as a function of period, as opposed to the patterns for Love waves, due to the medium layering. This is a medium effect and should not be confused with any pattern shape change due to the intrinsic properties of the source itself. As was the case for Love waves, there appears to be evidence of rupture propagation effects in the asymmetry of the pattern at short periods ( $T = 9$ seconds in particular).	13

LIST OF FIGURES (Cont'd.)

Figure Title	Figure No.
The theoretical Love to Rayleigh (L/R) wave ratio for Fallon, at $T = 16$ seconds, as a function of azimuth using the source parameters obtained for the results shown in Figures 12 and 13. Observations at various azimuths where the signal to noise ratios were high are indicated and identified by abbreviated station symbols. This shows the nature of the L/R azimuth variation for an earthquake in the same environment as the comparable explosion: SHOAL (see Figure 11). The L/R ratio for this event is much larger than that for the explosion at all comparable azimuths, except along nodal lines.	14
Surface wave spectra at 3 distances for the BILBY event. The points of observation are at approximately the same azimuth from the source. Note that the Rayleigh wave excitation is generally higher than the Love wave excitation.	15
Surface wave spectra at 3 distances for the Fallon event. The points of observation are at approximately the same azimuth from the source. Note that the Love wave excitation is generally greater than the Rayleigh wave excitation.	16
Surface wave spectra at 3 distances for the SHOAL event. The points of observation are at approximately the same azimuth from the source. The Love and Rayleigh excitation is of roughly the same order, although at the nearest (and most reliable) station the Rayleigh wave excitation is generally greater over the reliable period range.	17
Love wave spectra and spectral ratios for the SHOAL and Fallon events. The upper two graphs show the Love wave spectra for the individual events with the Rayleigh wave spectra given for comparison. Both spectra are individually normalized to unity at the maximum power point and the resulting normalized ratio of SHOAL to Fallon Love wave spectral density is plotted. The sampled spectral ratio is shown by the data points, the dotted curve is a smoothed fit to these sample points and the solid curve a $1/T$ curve given for comparison.	18

LIST OF FIGURES (Cont'd.)

Figure Title	Figure No.
Love wave spectra and spectral ratios for the BILBY and Fallon events. The upper two graphs show the Love wave spectra for the two events and the lower graph the normalized spectral ratio as described in Figure 18.	19
The variation of L/R versus period for the BILBY and SHOAL explosions and the Fallon earthquake, in the distance range near 800 km. The L/R for the earthquake is larger than 2 and increases with increasing period, while L/R for the earthquake is larger than 2 and increases with increasing period, while L/R for the explosions is between 1 and 2 and remains nearly constant with increasing period. This difference in behavior is a consequence of the much larger source dimension associated with the earthquake.	20
The variation of L/R versus period for the BILBY and SHOAL explosions and the Fallon earthquake, in the distance range near 1600 km. The L/R for the earthquake is again considerably larger than that for the explosions and increases with increasing period at this larger distance range, as expected. Note, however, that the details in the variation of L/R period, i.e., local maxima and minima, are considerably different than in Figure 20 and that the separation in the L/R is obscured at the short period end of the range.	21
The variation of L/R versus period for the BILBY and SHOAL explosions and the Fallon earthquake, in the distance range near 2800 km. At large distances the L/R separation between the earthquake and the explosions is maintained at long periods. The peak in the spectral ratio for Shoal at 30 seconds is probably due to a path effect.	22

## LIST OF TABLES

Table Title	Table No.
Description of data samples used	I
Source Parameters for Best Fit to Surface Wave Radiation Patterns	II

## INTRODUCTION

The surface waves radiated by explosions and by earthquakes are of special interest since they provide information about the intrinsic character of the source and the propagation medium. In this study we attempt to answer the following questions: first, what are the spatial radiation patterns from earthquakes and explosions, and how do they differ? Second, what are the differences between the long-period seismic radiation from these two types of sources, as determined from the surface wave spectra?

These questions are related to the problem of discrimination between the source types, and are comparative in nature. In addition to considering these questions, we also attempt to provide a theoretical explanation for the observed differences, and a quantitative description of the individual source properties.

Since this is primarily a comparative study intended to show differences between earthquakes and explosions, it is desirable to have at least one earthquake-explosion pair with a common origin point and common recording stations, so that the effects of propagation can be minimized. Ideally the sources should also be matched in radiated energy, so that a simple direct comparison can be made without the necessity for corrections which are complicated and perhaps not completely understood.

Of course, these conditions are impossible in practice; the closest we could come to meeting them was to use records from the Long Range Seismic Measurement (LRSM) station network, which provides good azimuthal and distance coverage from the Nevada Test Site, with well-calibrated sensitive instruments; we also chose an earthquake matching one of the explosions as closely as possible in location and magnitude. We found that an appropriate event pair for this purpose is the SHOAL explosion and the earthquake of 20 July 1962 at Fallon, Nevada. The parameters of all the events used in this study are given in Table 1. It is seen that the desirable criteria described above are reasonably well fulfilled.

Since we are interested in the nature of the explosion source, we also consider the BILBY explosion, which was well-recorded and of reasonably large magnitude. We compare this explosion with SHOAL in order to verify that the observed properties of the radiation from SHOAL are typical of other explosion events, and also to judge the variation of these properties with changing yield and source medium.

Figure 1 shows the location of the sources and the stations. It is evident that many of the receivers have a common propagation path for the SHOAL and FALLON events. Figure 2 shows the response of the long-period instruments

at the LRSM stations. The frequency range in which the signal-to-noise ratios required for this research were deemed adequate is indicated by the horizontal bar; all spectral data were corrected for instrument response within this range, and data outside this range were rejected.

Unfortunately, the azimuthal coverage of stations toward the west of the sources is rather sparse, and therefore some of our fits to the azimuth-dependent data must be regarded as tentative. Nevertheless, a large amount of data is available, and we can support our specific (albeit tentative) conclusions by a reasonably good general agreement with our theoretical predictions.

Part of the theoretical framework of this study is based on the work of Archambeau (1968; 1971). Briefly, this theory provides a description of tectonic effects in terms of an initial-value formulation, taking into account the initial stress field and its relaxation during the rupture process. Sources of this type are therefore termed relaxation sources. A discussion of the theory in the context of the present study is given by Archambeau (1971) in greater detail than we need present here. The present application of the theory is two-fold: first, as a means of guiding the development of this study and in interpreting the observations from the earthquake source; second, as a framework for the

interpretation of the anomalous radiation from explosive sources, which we consider to be of tectonic origin. In a later section the relevance and application of this theory will be discussed in greater detail.

## SIGNAL ANALYSIS

We have studied the surface wave radiation from the three seismic events, using a digital computer program which measures both the amplitude spectrum and the dispersion of the surface waves. This program is based on programs originally written by Alexander (1963), and is described in detail by Archanbeau and Flinn (1965). The program automatically performs a sequence of operations, ultimately giving the signal group velocity and amplitude spectrum. The amplitude spectrum is compared to a sample of noise preceding or following the signal, and the program flags and deletes from further analysis the period ranges in which the signal-to-noise ratio is too small to allow meaningful interpretation of the signal spectrum. The group velocity is calculated using a comb of narrow-band recursive digital filters (Archanbeau and Flinn, 1965). At each of many closely spaced frequencies the signal data window is passed through a narrow-band phaseless digital filter ( $Q = 500$  in this study; for background see also Rader and Gold, 1969). The envelope of the filter output at each frequency is calculated, and the time of occurrence of the largest maximum in the envelope is picked. This maximum occurs at the group arrival time (i.e., the energy arrival time) of the dominant mode present at that frequency. The epicentral distance divided by this time is thus the

apparent group velocity of the dominant mode, at the center frequency of the filter. Group velocities of secondary envelope maxima are also detected and displayed.

The variation with frequency of the amplitude at the time of occurrence of the dominant mode arrival gives an estimate of the amplitude spectrum of the dominant mode, and this therefore provides a method for determining surface wave mode spectra as a function of frequency. We call such spectra group spectra. These can be determined for each mode present at a given frequency. Figure 3 shows examples of raw data and the group velocity curves determined by the program. Figure 4 shows a comparison between the ordinary Fourier amplitude spectra and the group spectra. We have found in general that the two estimates agree to within a few percent in the frequency range in which the signal-to-noise ratio is greater than 1.5, even when more than one mode is present. We believe the group spectrum to be intrinsically more reliable than the Fourier spectrum, since we can associate a group arrival time with each spectral estimate, and thus eliminate those points in the spectrum which are badly contaminated by noise. We have therefore used the group spectral estimates consistently in the present study.

To calculate the theoretical Love and Rayleigh spectra, it is necessary to make some assumption about the velocity structure in the vicinity of the source. For the structure near BILBY we used model 35CM2 of Alexander (1963). For SHOAL and Fallon we used the structure previously used by Toksöz et al. (1965), which is a modification of Eaton's (1963) structure between San Francisco and Eureka, Nevada.

## CONCEPTS AND THEORY

An important concept underlying the theoretical framework of this research is that the radiated elastodynamic field, outside the region containing the source, can be represented in the frequency domain by a superposition of multipole contributions. This fact, familiar in the analogous cases of potential theory and electrodynamics, was formulated by Archambeau (1968) for an elastic radiation field. The implication is that we can represent the source of the radiated field as an equivalent point source located anywhere inside the actual region of energy release, and we can adjust the multipole coefficients so that the observed field outside the source region is identical to that caused by the true source. Since the multipoles are individually equivalent to particular superpositions of point forces, we can (if we wish) speak of force couples, double couples, etc., instead of multipoles, quadrupoles, and so forth. In the present study we discuss the equivalent point source for either the explosions or the earthquakes in terms both of the appropriate multipoles and their point force equivalents, depending on which designation is more familiar and useful in the particular context.

For the purpose of this report we will merely summarize the properties of the theory for the specific cases of interest, and then use these properties in the particular applications we wish to make. More detail on the theory is given in Appendix I.

I. For the shock-induced spherical shatter zone, the tectonic field is a pure quadrupole (double couple) field, and the frequency dependence of this quadrupole field is similar to that of the monopole component caused by the explosion itself, since the source dimensions are similar. The spectra for both source components are both quite sharply peaked at nearly the same frequency, and the spectra fall off with similar shapes on both sides of the peak (see Archambeau, 1971, for further details). These general results hold both when the rupture velocity is less than or equal to the shear velocity.

II. For the propagating spherical rupture, which we adopt as our model of the earthquake source at frequencies sufficiently low that the wave length of the radiated wave field is considerably larger than the rupture dimensions, the quadrupole or double-couple terms heavily dominate the solution, and the field is essentially pure quadrupole. At higher frequencies the higher-order multipoles can become comparable in amplitude. This is a result of the rupture propagation effect, and these multipole contributions are such that the spectrum has a sequence of maxima and minima at high frequencies, and the spatial radiation

pattern is more complex than that for a pure quadrupole pattern. In particular, the pattern has the general form of a quadrupole pattern but with larger amplitudes either in the direction of rupture propagation or in the opposite direction (see Archambeau and Minster, 1971, for details). The spectrum of surface waves from this type of source has an absolute maximum, the location and amplitude of which is controlled primarily by the length of the zone swept out by the propagating rupture. The average falloff of the spectrum on both sides of this peak is not as steep as for either the individual monopole or quadrupole components of the spectrum of surface waves from an explosion.

In view of these results we will use the following approach in the interpretation of the explosion and earthquake radiation fields:

(1) An explosion in a prestressed medium will be represented by superposed monopole and quadrupole fields. Since the quadrupole field is equivalent to a double-couple point force system, we will adopt the force equivalent convention in discussing the tectonic component of this source. We see from our previous discussion that if the higher-order multipoles are of tectonic origin, the quadrupole component will be essentially the only term worth considering for Love waves at long periods. Since we will analyze the surface wave radiation in the "long" period range, then whatever type of tectonic

effect is involved -- whether triggering of a linear rupture or simple relaxation around the shock-induced shatter zone -- the quadrupole field will still be dominant.

If induced faulting on a large scale does occur, then we would expect to see rupture propagation effects at the short-period end of our spectra. Further, if such triggering occurs, the pattern shape for Rayleigh waves at long periods should appear to be nearly an ideal quadrupole pattern rather than a superposed quadrupole-monopole pattern, since the quadrupole excitation for large-scale faulting will be considerably greater at very long periods than will the monopole excitation due to the explosion, simply because of the difference in source dimensions for the two source types. If the anomalous component of the field is associated only with relaxation around a roughly spherical shatter zone, the Rayleigh wave radiation pattern should have nearly the same shape over the entire frequency range of observation because of the similarity in multipole spectral excitation for the two source types; and the entirely anomalous Love wave pattern should not show rupture propagation effects: it should be pure quadrupole. We will examine the spectral observations from two explosions with a view to ascertaining which of these mechanisms is operative in a given case. Of course, we will also entertain the possibility that the anomalous field is not tectonic at all, but is conversion

due to cracking or non-parallel layering. In this study our main argument for acceptance of tectonic release rather than conversion is the quality of the fit to the observations that this hypothesis furnishes. At the very least, the observational data can be taken at face value, and we can argue that we have quantitatively determined the first two multipole contributions, whatever their origin might be.

(2) The quadrupole component of the surface wave radiation from the earthquake will be studied quantitatively. Hence we represent the earthquake by a double-couple point source, and as we have already seen, this will be the appropriate representation at long periods. At the short-period end of the surface wave spectrum we may anticipate seeing higher-order multipole effects due to rupture propagation. Since our range of observations is at rather long periods, the double-couple source will turn out to provide an appropriate spatial radiation pattern which can be used to fit the observations. Depending on the rupture length, however, we might expect to see departures in the radiation pattern from the pure quadrupole type, as well as the series of maxima and minima toward the short-period end of the spectrum, due to rupture propagation. We shall therefore check our observations with this in mind, although in the present study we make no attempt to fit the details of the source spectrum, nor try to study the effect of higher-order

multipole terms in the radiation patterns. Rather, we simply fit the spatial radiation pattern up to the quadrupole term, and draw conclusions from the nature of the fit. We then qualitatively compare the details of the observed spectrum and the observed spatial radiation patterns to the theoretical predictions.

Since we will deal in detail with monopole and quadrupole fields in this study, it is convenient to introduce parameters related to their force equivalents. For the double couple (the quadrupole equivalent) we define a plane along which one of the couples is oriented, the other couple being oriented in a direction perpendicular to it. Figure 5 shows such a plane, with its orientation in space specified by the unit vectors shown. For an earthquake, this plane corresponds to the fault plane, which is simply a limiting form of the surface enclosing the region of failure. If this region has a small width relative to its other dimensions, there is little geometrical distinction to be made between the envelope surface and the fault plane shown in Figure 5.

As is customary, the orientation of the fault plane is described by a strike angle, measured from north, and a dip angle measured from the normal to the strike direction, as shown. A point of observation (O) will be specified by an azimuth angle  $\theta$ , measured from the strike direction, and an

epicentral distance,  $r$ , measured from the point of initiation of the rupture; this latter point is shown in Figure 5 as the origin of coordinates. If the fault plane or actual rupture surface may terminate at some depth  $h$  below the earth's surface, this distance is measured in the direction of axis  $x_3$  in Figure 5, normal to the surface of the earth.

We define  $\underline{t}^{(0)}$  in Figure 5 as the traction vector at a distance  $-c/2$  just behind the fault plane, when the fault plane is viewed from the direction defined by  $\hat{n}$ . When the fault plane is approached from the  $-\hat{n}$  direction there is an equal and opposite traction  $-\underline{t}^{(0)}$  at a point a distance  $+c/2$  just in front of the plane. This configuration of tractions defines one of the force couples for the equivalent source; its orientation in the plane will be described by the so-called slip angle, which is simply the angle  $\lambda$  defined with reference to  $\underline{t}^{(0)}$ , as shown in Figure 5. For the full quadrupole equivalent we require an equal and opposite couple whose orientation is perpendicular to the plane shown in Figure 5, such that the net torque at the point  $P$  is zero. This particular configuration is required by the equilibrium equations, since for a relaxation process no net torques can be maintained. The origin of the second couple is the Poisson effect which occurs during relaxation.

In the case of an earthquake the definition of the fault plane and the system of couples just described is intuitively

appealing and reasonably straightforward (although from a purely intuitive approach, only a single couple might appear to be required at first sight; this fact has contributed to the well-documented disagreement among seismologists as to whether a single or double couple source is required). For stress relaxation associated with a "spherical" shatter zone, however, the same equivalent double-couple point source applies, but of course the physical identification of a "fault plane" is no longer obvious. Even so, we will define a plane through the source and its associated orientation parameters for this problem as well. In this case, which may apply to explosion-generated earthquakes in the real world, the plane and the couple orientations are related to the orientation of the prestress field.

This approach allows us to use Ben-Menahem and Harkrider's (1964) point source results directly, to describe the quadrupole field from an earthquake and from an explosion in a stressed medium. Since we are primarily interested in theoretical fits to the azimuthal dependence of the radiation fields, we need only calculate the variation of a single function,  $\chi(\theta)$  which gives the radiation patterns for either Love or Rayleigh waves from a double-couple point source at a depth  $h$  in a plane-layered earth model. In particular, Ben-Menahem and

Harkrider (1964; equation 25) give:

$$\chi(\theta) = d_0 + i(d_1 \sin \theta + d_2 \cos \theta) + d_3 \sin 2\theta + d_4 \cos 2\theta$$

where for Rayleigh waves the coefficients are:

$$d_0 = 1/2 B(h) \sin \lambda \sin 2\delta$$

$$d_1 = -C(h) \sin \lambda \cos 2\delta$$

$$d_2 = -C(h) \cos \lambda \cos \delta$$

$$d_3 = A(h) \cos \lambda \sin \delta$$

$$d_4 = -1/2 A(h) \sin \lambda \sin 2\delta$$

and for Love waves the coefficients are:

$$d_0 = 0$$

$$d_1 = G(h) \cos \lambda \cos \delta$$

$$d_2 = -G(h) \sin \lambda \cos 2\delta$$

$$d_3 = 1/2 \sin \lambda \sin 2\delta$$

$$d_4 = \cos \lambda \sin \delta$$

The functions  $A(h)$ ,  $B(h)$ ,  $C(h)$ , and  $G(h)$  depend on the equivalent point source depth and on the details of the earth model chosen. They are given explicitly by Ben-Menahem and Harkrider (1964; equations 26-36), but since they are quite

lengthly, they will not be reproduced here. We will vary  $\nu$ ,  $\delta$ ,  $\phi$ , and  $h$  to fit our observations, while maintaining a fixed average crust-upper mantle model appropriate to the western United States in the remainder of this work. Without detailed path corrections (or control), therefore, we expect to see scatter in the observations about any fit we might achieve, and this will to some extent limit our ability to draw hard conclusions. However, with a good average structural model we can expect to resolve and identify all but the more subtle radiation pattern variations.

For the monopole field from the explosion we merely note that it has the form (in our present notation):

$$\chi_{\alpha}^{(2)}(\underline{r}, \omega) = \Lambda_{00}^{\alpha}(\omega) h_0^{(2)}(k_{\alpha} \tau)$$

with

$$\Lambda_{00}^{\alpha}(\omega) = \begin{bmatrix} 0 \\ 0 \\ 0 \\ G(\omega) \end{bmatrix}$$

The function  $G(\omega)$  will depend on the radius of the elastic-plastic boundary and the effective pressure at this radius. Archanbeau (1971) describes such functions and the various ways of determining them. It is clear, however, that we can

again use a point source model and employ Ben-Menahem and Harkrider's results for a point pressure source without being directly concerned with all the details of the function  $G(\omega)$ .

In particular, our procedure in dealing with the explosion is to superpose a point pressure and point double-couple sources and to scale the double-couple component by a factor  $F$  (see Toksöz et al., 1965). For observations of the radiation pattern at a given frequency, then, we can adjust this factor  $F$ , along with the other parameters of the double couple, in order to obtain a theoretical fit to the observed radiation pattern. If  $G(\omega)$  is such that the actual source monopole spectrum is similar to the quadrupole spectrum over the range of observation, then the fit achieved at one frequency should hold over the entire frequency range. If the monopole excitation is quite different from that associated with the quadrupole term, then the  $F$  factor will change with frequency. From our earlier discussion of the effects of shock-induced relaxation we note that if relaxation around the shatter zone is all that is involved tectonically, then the  $F$  factor, once determined, should be found to remain fairly constant with frequency. If triggering of large-scale asymmetric faulting is involved, the  $F$  factor should increase strongly with increasing period,

reflecting greater quadrupole excitation at long periods. Thus we will attempt to fit radiation patterns over a range of frequency in order to determine whether such variations in  $F$  exist\*

To conclude this part of our discussion, it is worthwhile to note some of the less obvious difficulties inherent in fitting theoretical predictions to the observations. These difficulties arise primarily from a lack of uniqueness in fitting the observations, and are best illustrated by a few examples.

In particular, since the azimuthal variation of the ratio of Love to Rayleigh wave amplitudes ( $L/R$ ) at a given frequency is an important variable, it is appropriate at this point to discuss the effect on the  $L/R$  radiation pattern of variations in the free parameters describing the source. For an explosion with an anomalous quadrupole or double-couple component, we have as variables the depth of the double couple; the strike, dip, and slip angles describing the orientation of the double couple; and the  $F$  factor relating the monopole excitation to the quadrupole excitation. We note parenthetically that the depth of the equivalent double couple required to explain the observations could,

---

\*We note also that intuition suggests a roughly constant  $F$  value if conversion by cracking causes the Love waves.

if it is significantly different from the known depth of the explosions, be diagnostic of the mechanism of the quadrupole field: a much greater depth, for example, would suggest triggering of an earthquake, while a depth near that of the monopole equivalent might be caused either by triggering or by relaxation due to the shatter zone itself or by conversions.

For an earthquake we have the same parameters available except for the  $F$  factor, since for earthquakes we assume that there is no monopole contribution.

Many variations of combinations of these parameters can give rise to closely similar L/R patterns. Figure 6 shows, for example, the variation in L/R pattern for an explosion in a stressed medium for different double-couple slip angles. A similar variation in the pattern, involving slight azimuthal rotations and changes of magnitude, can be caused by changes in the depth of the double-couple component. Similarly, radically different values of slip angle and double-couple depth equivalent can result in the same observed radiation pattern. A similar ambiguity exists in the combination of dip angle and the  $F$  factor for an explosion. Figure 7 shows the variation in the L/R pattern for varying dip angle, holding the other parameters fixed. Here the pattern lobes increase in magnitude with increasing dip, and essentially the same kind of variation occurs as  $F$  increases.

Furthermore, various combinations of strike, slip, and dip angles, and the F factor can be found that give very similar radiation patterns, so that we are confronted with the fundamental lack of uniqueness which is characteristic of most geophysical problems. In our treatment of the actual observations and the theoretical fit to our data, we therefore work in a period range in which the scatter of data is small, so that we can with reasonable justification make relatively fine distinctions in the fitted models. We also constrain our solutions to be in at least rough agreement with the known tectonic setting of the source area: thus we make use of the fact that something is known of the strikes and dips of the faults in the source region, and we impose a set of constraints on our allowable source models. Further, the ambiguities for the earthquake are not as serious as for the explosions, since we deal with only one type of equivalent source, and we use the fit for the double couple of the earthquake as a guide for possible solutions for the SHOAL explosion. This presupposes tectonic release as the origin of the double-couple component, of course, and hence only serves to constrain permissible solutions of this type.

## SURFACE WAVE RADIATION PATTERNS AND DEDUCTION OF THE EQUIVALENT MULTIPOLE SOURCE

In this section we consider the surface wave radiation patterns associated with the two explosions and the single earthquake studied, and discuss the point-source models implied by the data.

Figure 8 shows Love and Rayleigh wave patterns for two BILBY explosion frequencies spanning the bandwidth in which the signal power was greatest. We note that the stations closest to the sources give an adequate azimuthal coverage for our purposes, although more stations to the west would have been desirable. It is reasonably clear that variations in crust and upper mantle structure strongly perturb the radiation patterns; in particular, the stations in the eastern United States show quite large amplitudes which consequently cause distortions in the contours of the pattern. It appears that eastward-propagating surface wave energy, once across the Rocky Mountains, propagates from there on with little attenuation, and that the observed surface wave amplitudes can actually be greater in the East than at stations in the western tectonic provinces which are much closer to the source. This can be explained in part by the fact that the crust in the eastern United States has intrinsically higher wave

velocities in the intermediate and deep layers than does the crust in the Basin and Range Province (see, for example, Archambeau et al., 1969). The top of the upper mantle also has higher velocity in the East than in the West. This results in a distribution of the surface wave energy nearer the surface for surface waves in the period range observed (5 to 40 seconds), and hence higher amplitudes at the surface, even though the total wave energy is less. Further, the lateral variations within the eastern provinces appear to be milder than those in the tectonic provinces in the West (Archambeau et al., 1968, 1969) and hence there is less scattering and more uniform propagation of the waves generally.

The patterns in Figure 8 for both Love and Rayleigh waves can be approximated by superposed quadrupole-monopole sources with both equivalent point sources at the depth of the detonation point for the explosion. These theoretical patterns, approximately the same for  $T = 15$  or  $20$ , are shown in the insets in Figure 8. The source parameters are as given in the figure and listed in Table II; the ellipticity parameter  $\epsilon$  is determined by the structure used to predict the radiation patterns. We were particularly interested in the effect of varying the depth of the double couple equivalent, but found that the best fit to the observations is given by a double couple at the depth of the explosion. This supports a local effect such as

tectonic release or conversion in the very near vicinity of the explosion, but does not clearly distinguish between induced faulting as opposed to relaxation due only to the shock-generated "spherical" fracture zone.

It is also significant that the same combination of monopole and quadrupole sources fits both the Love and Rayleigh waves. Further, we found very large changes in observed amplitudes of the radiation patterns between two frequencies where the shape of the pattern remains essentially invariant. In addition, the pattern did not vary significantly from that shown over the entire range from approximately 10 seconds to 35 seconds, although at the extremes of this range the observed power was low and the pattern resolution became poor. Nevertheless, we conclude that there is no evidence of pattern shape change over this range. This supports the idea that the mechanism associated with the double couple source is not only located in the near vicinity of the explosion, but that the spectrum produced by this mechanism is similar in shape (as a function of frequency over the range observed) to the explosion spectrum. Indeed, the scaling factor  $F = 0.5$  for the double couple is independent of frequency over the observed range, as is predicted for the radiation due to relaxation around the shock-created shatter zone. The magnitude of this excitation factor is also of the order expected for relaxation.

The amplitude and energy spectrum produced by this double couple source component from Bilby has been studied by Archambeau and Sammis (1970) under the hypothesis that this contribution to the field is actually due to tectonic prestress relaxation around the shock-induced shatter zone. It was found that a fit could be achieved for a homogeneous shear prestress of 70 bars and a shatter zone of roughly 400 meters in radius, which are reasonable values. Thus we tentatively conclude that the observations from BILBY support the hypothesis for this particular form of tectonic release. We do not see a change in pattern shape as predicted for large-scale faulting, and while we cannot definitely rule out a triggering effect, there is little evidence to support it. Aki et al. (1969) have, however, drawn the opposite conclusion based on a different set of observations.

As to the fundamental question of whether tectonic effects are responsible for the double couple component, we note at this point that the strike and dip of the "couple plane" ( $\phi = 342^\circ$ ,  $\delta = 90^\circ$ ) are consistent with the orientation of tectonic features in the vicinity of the explosion site. This simply indicates that the average stress field in the region is oriented so as to produce a double couple field in agreement with the observations for either fault triggering or shatter-zone relaxation effects -- therefore, the tectonic hypothesis is at the very least consistent

with our observations. Furthermore, while our amplitude pattern fit indicates a double couple source in the near vicinity of the explosion (within a few kilometers), observations of the Love wave group velocity requires that the double couple be very close to the explosion site, in order that the observed group velocities be compatible with our rough knowledge of the crustal structure along the propagation paths. Hence, while one might argue from the observations of the Rayleigh waves alone that the patterns might be accounted for by amplitude fluctuations caused by local structural variations at the individual stations, it is impossible under such a hypothesis to explain the Love and Rayleigh wave group velocity observations, which are consistent with our prior knowledge of source-to-station velocity structure within the Basin and Range Province. In particular, only a double couple source at the explosion location can explain all our observations.

The theoretical patterns shown in Figure 8 provide a rather qualitative way of fitting the observations; that is, we have tried to fit by comparing the general shapes with the contours obtained from the observations. A more quantitative approach is achieved by the method illustrated in Figure 9. In this case we can simultaneously consider Love and Rayleigh wave amplitude patterns (the vertical component amplitude in the case of Rayleigh waves) by fitting their ratio, which we will designate

as L/R. This can be done as a function of frequency, so that we consider a reasonable frequency sampling of such L/R patterns and fit them with a fixed combination of monopole and quadrupole parameters. The parameters are the same as for the patterns shown in Figure 8 and listed in Table II, of course, and we only note that the L/R fit can be seen to be quite good. All the source parameters listed remained nearly constant over the range 10 to 35 seconds. We will return to the spectral character of the L/R ratio in the next section, but at this point it is reasonable to strongly suspect that the mechanism producing the double couple component for BILBY is tectonic stress relaxation near the roughly spherical shatter zone, because of this constancy of source parameters versus frequency.

The SHOAL explosion was considerably smaller than the BILBY event (Table I), but a double-couple component similar to that obtained for BILBY was observed. In particular, Figure 10 shows radiation patterns similar in shape to those observed for BILBY and the theoretical fit achieved gave an F factor and double couple source depth which are like those for BILBY. The same interpretation follows; that is, the stability, or shape invariance, of the patterns with frequency (over the range 10 to 30 seconds in this case), the coincidence of the quadrupole and monopole source depths, the strike and dip of the equivalent "fault" plane coinciding with tectonic features of the area and

the moderate constant value for  $F$ , all imply tectonic release due to stress relaxation near the explosive shatter zone. Further, the source parameters defining the double couple component are nearly identical with those obtained for Bilby, which implies a similar tectonic stress field in the two areas\*.

Figure 11 shows the L/R pattern at a period of 15 seconds. The fit to the data is quite good considering the large variance to be expected in the ratio of two spectra, due, for example, to structural effects and noise. The scatter from the theoretical fit would also manifest itself in the form of displacements of the observed points on this plot in azimuth, due to refraction of the surface waves as a consequence of lateral variations. Lateral variations in structure have not, of course, been taken into account in the theoretical calculations. These effects are quite apparent in Figure 10, however, and it is easy to see that in the vicinity of the epicenter the pattern most closely approaches the theoretical pattern, while at greater distances the energy has been refracted and scattered by velocity gradients along the path so as to distort the basic symmetry observed near the source. We note that the effects of lateral variations in structure on the pattern shapes will be frequency-dependent, and Figure 10 illustrates this fact.

---

\*Of course the possibility of conversion due to cracks controlled by the local stress field cannot be ruled out.

One of the major considerations of this study is the comparison of an earthquake field with those from the explosions. The Fallon earthquake was located very near to the SHOAL epicenter and so a comparison with SHOAL is most straightforward.

Figure 12 shows the Love wave radiation patterns from the Fallon earthquake; the inset shows the double couple equivalent which gives a best fit to these observations. The same equivalent was used to fit the Rayleigh wave patterns and the L/R data as well, of course. The parameters for this equivalent are to be compared to the double couple parameters obtained from the SHOAL explosion. The most significant difference between the double couple equivalents for the two sources is the difference in depth of the earthquake double couple. In view of the reasonably strong constraints placed on depth by the radiation patterns, we are confident that an appreciable difference in depth exists. We therefore have an example of what a triggered event at depth would contribute to the surface wave radiation from an explosion. Here we note that the earthquake has a significantly lower body wave magnitude than the explosion (Table I) and hence is energetically of the size and at a depth that has been hypothesized for triggered events associated with explosions in the range of SHOAL and BILBY. We immediately note, however, that beside the fact that an

equivalent double couple at the surface fits best to the explosion data rather than one at significant depth, it is also evident that the double couple for the earthquake has a much higher excitation in the 10 to 30 second period range than does that for the explosion. This is evident by comparison of the Love wave amplitudes for Fallon with those for SHOAL and is even clearly true for BILBY which is more than an order of magnitude larger energetically than Fallon. Thus, we would expect that if a triggered earthquake occurred with the explosions that it would have characteristics very similar to the Fallon earthquake, especially, of course, for the SHOAL explosion. However, we see that the observed characteristics of the anomalous double couple components associated with the explosions are very different from those of the earthquake, and conclude in accordance with Archaubeau's theory that the most probable mechanism is tectonic release associated with the highly symmetric fracture zone created by the explosive shock wave.

One other important conclusion to be drawn from the difference in the long-period double couple excitation of the earthquake relative to the explosions is the fact that we can quite easily distinguish between earthquakes and explosions just on the basis of the Love wave excitation relative to  $m_b$ , down to  $m_b \sim 4.4$ . This, of course, has been observed

before (Evernden, 1971), at least indirectly, in terms of  $m_b$  vs.  $M_S$  differences. While it is clear that caution is necessary, since we are considering only one earthquake which may have somewhat special characteristics, it seems quite unlikely that these differences would change very radically with decreasing magnitude. Thus we expect to see differences in the quadrupole components of earthquakes and explosions, especially in the Love wave excitation, down to  $m_b$  magnitudes below four for most if not all earthquake-explosion pairs. We shall discuss this point again in the next section, where we will consider these inherent source differences in terms of Love to Rayleigh wave spectral ratios.

Another aspect of the comparison between the quadrupole components of SHOAL and Fallon is the similarity in the orientation of the equivalent double couples. We expect that if the origin of the Love waves for the explosion is tectonic stress relaxation, then the orientation of the double couple equivalent for the explosion should be similar to that for the earthquake, provided of course that the prestress field is reasonably well-behaved and such that averages taken over volumes of the order of kilometers in diameter do not vary much in this region. We observe from comparison of the parameters describing the double couple equivalents for the

explosion-earthquake pair, as illustrated by the insets in Figures 10 and 12, respectively, that there is a strong correlation of the double couples in terms of their orientations, although there is a large difference in their relative magnitudes. This is consistent with the idea that tectonic relaxation of a regional stress field was involved in both cases, and that the earthquake was much more efficient at low frequencies.

If we examine the radiation patterns shown in Figure 12 in more detail, we see that the theoretical quadrupole pattern shown is a rather rough approximation to the observations, although a good first-order fit. There are at least two possible reasons for this: first, we expect rupture propagation effects to distort the patterns at wavelengths comparable to the rupture length in the manner described earlier; second, we expect structural variations to cause perturbations in the patterns. Both effects appear to us to be present here. Note in particular the distortion of the pattern at  $T = 9$  seconds; the amplitudes on the NE lobe of the pattern appear to be 3 to 4 times as large as those within any of the other lobes. This effect is seen to diminish rapidly with increasing period. We consider this deviation from a pure quadrupole pattern to be predominantly due to rupture propagation, although we cannot definitely rule out

structural focusing effects. Although the amplitudes were low at short periods for the SHOAL event, we did not see similar effects; and if either structure or fault triggering were involved in large measure, such a distortion should have been evident.

Structural effects are obviously strong, however, and we note that, as with the observations of SHOAL and BILBY, surface waves propagate efficiently east of the Rocky Mountains. It is worth noting that the contour pattern swings away from north toward south with increasing period in the eastern part of the continent as well. This implies that in the north there is a higher velocity in the lower crust and upper mantle compared to the south; or at least, such a variation is consistent with this sort of refraction effect; this agrees with our knowledge of the structural variation in this part of the continent.

Figure 13 shows the Rayleigh wave patterns from Fallon along with the theoretical pattern produced by the same quadrupole used to fit the Love waves. In this case, because of the orientation of the equivalent double couple, the pattern shape changes with frequency. We observe a rather remarkable first-order agreement between the theoretical and observed patterns, particularly when we consider the combined Love and Rayleigh wave data. Again we observe strong perturbations in

the patterns due to structure, especially in the east. However, close to the source we again observe what appears to be evidence for rupture propagation in the distortion of the pattern, resulting in larger amplitudes to the north at short periods. Again a strong conclusion to this effect is not possible, but at least the Love and Rayleigh waves both show the effect, as would be expected if it were due to rupture propagation.

In the east the effects of lateral structural variations are different for the Rayleigh waves than for Love waves in that we observe no similar rotation of the pattern from north to south for Rayleigh waves. However, the Rayleigh wave excitation is smaller, and noise may obscure the true behavior of the pattern as a function of period.

A composite picture of the fit to both the Love and Rayleigh wave radiation is provided by the fit to the Love to Rayleigh spectral ratio. Figure 14 shows the L/R radiation pattern at  $T = 16$  seconds, a period of high amplitude for both types of surface waves. Considering the combined effects of lateral structural variations and rupture propagation as perturbing influences, the simple quadrupole pattern shown gives a remarkably good fit to the data. The important point here is that the L/R ratio for Fallon is much larger than

the L/R ratio for SHOAL, and this is true at every azimuth with the exception of only those (singular) points along the node lines. This may thus potentially be a useful discriminant between explosions and earthquakes, especially if it holds over a wide period range. In the next section we will investigate the period range over which this difference applies; we will see that for observations at larger distances, it is necessary to consider the L/R ratio at progressively lower frequencies in order clearly to distinguish between the two source types on the basis of larger L/R for earthquakes. Nevertheless the difference holds.

#### Spectral comparisons

In the previous section we focused most of our attention on the azimuthal variation of the fields from these sources, and to some extent on their distance dependence. In this section we look more closely at the spectral properties of the files. It is, of course, important to keep in mind that the spectral characteristics vary with azimuth and distance, and we will therefore attempt to integrate the results of the previous section with the present discussion.

Figure 15 shows observed surface wave spectra from BILBY at progressively larger distances along a line of stations at roughly the same azimuth. The radiation patterns for BILBY show

that stations along this azimuthal sector lie near the maximums of the quadrupole lobes for both Love and Rayleigh waves. These spectra show that the Rayleigh wave excitation is generally greater than the Love wave excitation over the range of observations from 5 to 40 seconds, and that the observed spectra peak in a range near 10 seconds period. The exception to these generalizations is the Love wave spectrum at BX-UT, which shows an increase in amplitude in the 30 to 40 second period range. Since the time sample used to obtain the spectral estimate at this near distance range was short (the signal being quite pulse-like), so that corrections for sample trend and the like are therefore more uncertain, we feel that this feature in the spectrum may be an artefact of our procedure.

The BILBY spectra can be usefully compared with the Fallon earthquake spectra shown in Figure 16. We see that for Fallon the Love wave spectra are generally greater than the Rayleigh wave spectra at all distances, which is opposite to the relation for the explosion, and that the spectral peak is in a range near 20 seconds, although the Rayleigh wave spectrum does not have a very clearly defined absolute maximum. In any case, even a casual comparison of the spectral characteristics of the surface wave spectra from the two source types shows that the Love wave excitation from the earthquake is relatively much greater than from the explosion and that the spectral

excitation is shifted toward longer periods. Much of the detailed character of the spectra shown is of course controlled by the structure; however, source spectral characteristics appear to result in changes in the gross properties just mentioned.

Figure 17 shows the comparable spectra for the SHOAL event. In general, the spectral amplitudes are rather low and therefore noise is a significant background effect. In particular, we regard the rise in the spectra beginning around 30 seconds and extending to the 40 second limit to be spurious and to be due either to imperfect knowledge of the instrument response at long periods, or ambient background seismic noise, or both. Ignoring this suspect part of the spectrum, we note that the spectra of both types of surface waves peak near 10 seconds (actually at periods somewhat less than 10 seconds as compared to BILBY, where the spectral maxima occur, on the average, at periods somewhat greater than 10 seconds). The Rayleigh wave amplitudes in this restricted period range are of the order of or greater than the Love wave amplitudes. Again we observe that the explosion produces surface waves with relatively greater excitation at short periods than does the comparable earthquake, but does not produce Love waves with anything approaching the same efficiency as a comparable earthquake.

A more quantitative means of comparing the frequency dependence of the Love wave excitation between an earthquake and an explosion is to calculate the ratio of the normalized Love wave spectrum for the explosion by that of the earthquake. Figure 18 shows the Love wave spectra for SHOAL and Fallon recorded over nearly identical paths. The spectral ratio for the Love waves should therefore be essentially independent of path and should reflect source differences directly. Furthermore, the Love wave excitation is a very slowly varying function of depth and, for a source depth difference of around 20 km for these two sources, will have a small effect (Harkrider, 1964); hence we see principally the spectral differences in the source equivalents themselves. The ratio shown in Figure 18 indicates the relatively greater short-period excitation of Love waves for an explosion relative to an earthquake of comparable magnitude.

In terms of a relaxational source, this would be explained in terms of a much larger source dimension for the earthquake than for the tectonic source associated with the explosion. This is consistent with the hypothesis of stress relaxation from the region around the shock-induced shatter zone. We might emphasize that even though the P wave magnitude of the earthquake was significantly smaller than the explosion, the source dimension appears to be substantially larger. We

have shown a  $1/T$  curve only for comparison with the data; however, we observe that where the power is high for both terms of the ratio, the data appear to fit such a dependence quite well. We will consider theoretical predictions of the relative Love wave excitation for explosion and earthquake models in a later study, with the objective of comparing these predictions, for various model types, to data such as these.

Since the power at the long-period end of the Love wave spectrum for the SHOAL explosion was low and probably contaminated by noise to a significant degree, we have plotted the sample spectral ratio for the BILBY-Fallon pair, since BILBY has reasonably high power in the 20 to 40 second period range. Figure 19 shows the results, with a reasonably close fit to a  $1/T$  dependence at the long-period end of the spectrum. Taken together, then, the spectral ratios for Love waves from these explosions relative to the Fallon earthquake appear to follow a dependence which is roughly  $1/T$  in the range which the observations are reliable. This merely quantifies, somewhat, our earlier statement that explosion-generated Love waves are predominantly of shorter period than Love waves from an earthquake of comparable magnitude (or energy). An explanation is of course that the source dimensions are quite different, the earthquake being the larger.

Perhaps the most interesting result of this study is that the Love wave excitation from the explosions is significantly different than that from the earthquake. This difference of course is expected for an idealized explosive source; the only question is how strong the anomalous effects might be in actual cases. We have seen that while the anomalous field appears to be tectonic in origin, it is not so overwhelming as to mask distinguishing properties of the purely explosion-generated field.

To summarize these differences, we again consider the Love to Rayleigh wave ratio (L/R) for these events. Figures 9 and 11 show the spatial character of this ratio for the two explosions and comparison with the ratio for Fallon in Figure 14 indicates the differences in these characteristics at a fixed frequency. We see that at nearly every azimuth the L/R ratio for the earthquake is large compared to that for the explosions and especially so along the strike of the "fault plane". This suggests that by checking the L/R spectral ratio at only a few stations we might be able to distinguish between earthquakes and explosion sources. It is important, however, to investigate the detailed behavior of this ratio as a function of frequency in order to see whether the difference holds over a wide range of frequency and whether there is some frequency where the difference is maximized. In particular, does L/R

for earthquakes remain large compared to that for explosions as the period increases? Also, can the difference in the L/R excitation for different small sources be distinguished at large distances?

In order to answer these questions we consider the L/R spectra at stations along a nearly constant azimuth to the east of the studied. This selection of azimuth does not maximize the difference between L/R for the earthquake compared to the explosions, as can be seen from again comparing Figures 9, 11 and 14; and is representative of the average difference likely to be seen over a distribution of stations rather than the extreme difference.

Figure 20 shows the L/R spectra at a relatively close range for the three events studied. It is clear that the closely related SHOAL-Fallon pair are very different, since the L/R spectra for SHOAL remains rather flat and near unity (actually less than unity), while that for Fallon is nearly three at the 10-second limit, increasing with increasing period and approximately an order of magnitude larger at 30 seconds period. Generally speaking, L/R for BILBY is similar to that for SHOAL, although on the average it is somewhat larger over this period range. Thus over the frequency range where the observations are reliable, L/R for the earthquake is much larger than for the explosions and increases with increasing period.

Figure 21 shows the L/R spectra for the events at an intermediate teleseismic range, at approximately the same azimuths as those in Figure 20. We note that roughly the same relationship between the events again holds. In this case, however, the spectral amplitudes for BILBY appear to be lower, on the average, than SHOAL. However, note that the distinction between the earthquake and the explosions in terms of L/R at the short-period end of the spectral range has been lost. This is probably due to the effects of structure, e.g., scattering from lateral variations. We also note that several maxima and minima occur in the spectra, whereas the spectra at the closer distance were more regular. Again we consider this to be associated with structural irregularities. This emphasizes the difficulties involved in isolating a spectral peak (or a minimum in the spectrum of the vertical component of the Rayleigh wave) which can be associated with a source depth effect. Markrider (1970) considers in detail the question of the effect of source depth on the L/R spectral ratio, using the Fallon earthquake as an example.

Finally, Figure 22 shows the spectra at a distance of nearly 3000 km from the sources. We note that the spectrum from Fallon has an L/R ratio which increases dramatically with period and actually extends to a value considerably larger than 20 at the longest period of the range. However, since the

observed power at the extreme end of the range was low for Fallon, we do not consider the data beyond 20 to 25 seconds to be very reliable. Nevertheless the spectrum maintains a much higher value than the explosions over a considerable period range. We also note that the SHOAL spectrum exhibits a large peak near 30 seconds period; however, the power was extremely low at this distance and at this period, and considering the noise levels and the effects of structure on such a spectral ratio, we conclude that this peak may very well be spurious.

Taken together, the last three figures, along with the radiation patterns shown for L/R earlier, show that the L/R ratio is larger for this earthquake than for the explosions over a period range from around 10 to 35 seconds. It is significant that this holds at all azimuths (the few exceptions being explained by nodes in the radiation patterns) and over the distance range from about 500 to 3000 km. The difference in the L/R ratio between this earthquake and the comparable explosion appears to increase with increasing period quite strongly, ranging from a factor of 2 or 3 difference near 15 seconds to a factor of around 10 near 30 seconds. Various maxima and minima appear in the spectra, depending on the distance of observation; these are most likely associated with scattering due to structural irregularities, the Love

waves being affected differently than the Rayleigh waves. This strongly suggests that determination of depth from spectral minima (or maxima) is probably decidedly difficult and perhaps not useful in a practical sense. This conclusion is consistent with that obtained by Harkrider (1970) in his detailed study of the surface wave spectra and L/R ratios from Fallon.

We conclude that the L/R spectral ratio may be a reliable discriminant for magnitudes near 4.5, and possibly to lower magnitudes. We have not, of course, demonstrated that this difference is appropriate for all earthquakes, and it is entirely possible that some earthquakes may have properties quite different from the one studied, and thus produce L/R spectra similar to that from explosions. In this regard, deep earthquakes, earthquakes of volcanic origin, and dip-slip faulting will probably not show such a strong L/R difference from explosions selected from arbitrary tectonic regions. However, it seems clear that for an explosion in a tectonic environment which produces dip-slip faulting, we would expect a corresponding and proportionate decrease in Love wave excitation (since such excitation is also due to a tectonic origin) as the earthquake, and hence for other events, within the same tectonic region an L/R difference between

explosions and earthquakes similar to that observed here for a region typified by strike-slip faulting. In any case, the use of the L/R spectral ratio as a discriminant appears potentially useful, but the possibility of practical application needs additional study, using a wider selection of earthquakes and explosions from different tectonic environments than that used here.

A second conclusion which can be drawn from the nature of the L/R spectra verifies that inferred from the comparison of only the Love wave spectra for the events as given in Figures 18 and 19. In particular, the increase of L/R with respect to period for the earthquake, and the generally higher value of this ratio over the entire period range compared to the explosions, indicates that the anomalous shear wave radiation from the explosion is consistent with a source mechanism which is of much smaller dimension than that of the earthquake. It is important to note here that the effect of the difference in source depth between the earthquake and the explosion (20 km) is such as to predict that the L/R ratio will have its largest difference at short periods, with the shallow source excitation being the greater, and that the L/R ratios become nearly the same at longer periods (30 seconds). (See Toksöz et al., 1965, Figure 6 and 13). This is just the opposite of what is observed, and hence the observation is probably due to an

intrinsic source property rather than a medium response effect due to depth of source. If we assume that the origin of the anomalous field, which manifests itself principally as Love wave radiation, is of tectonic origin, then we are led to conclude that the effect is due to stress relaxation around the shock created shatter zone, in view of the implied small dimensions of this source.

## CONCLUSIONS

We draw the following conclusions from this study:

(1) The earthquake radiation field is to first order a quadrupole field in the spectral range where typical wavelengths of the radiated field are larger than the rupture dimensions. At shorter periods there are indications, in both the radiation patterns and spectra, of higher order multipole contributions produced by rupture propagation. These results are in quantitative agreement with the theoretical predictions.

(2) Tectonic stress relaxation is by far the most likely origin of the anomalous contribution to the radiation field from the explosions. From our analysis of the spectral and radiation pattern observations, we conclude that the effect is most likely due to stress relaxation around the shock-generated shatter zone for the events studied.

(3) The anomalous field from the explosion is purely quadrupole over a wide spectral range. Since the Rayleigh wave radiation patterns do not change toward being a quadrupole type at longer periods, and since the Love to Rayleigh excitation ratio is near unity, we conclude that the source spectrum for the anomalous field is similar in shape to that for the explosive monopole component of the total field. This is in agreement with theoretical predictions for stress relaxation around the shock-generated failure zone.

(4) The spectral ratios of Love waves from the explosions, relative to the earthquake, show a long-period excitation for the anomalous explosion field which has a fundamentally different frequency dependence within the range of observation (10 to 40 seconds period): the anomalous explosion field has a frequency dependence resembling  $\omega^{m+1}$  (where  $m$  is some positive integer), while the earthquake spectrum has a dependence like  $\omega^m$ . Thus the ratio decreases as  $\omega$  with increasing period in this range. This implies that the source of the anomalous explosion field is quite different from the comparable earthquake, and we conclude that if the origin is tectonic, it is associated with a region of relatively small dimension. This suggests that these effects are due to stress relaxation around the shatter zone.

(5) The ratio of Love to Rayleigh wave spectral amplitudes generated by the sources studied here show that the earthquake ( $m_b = 4.4$ ) excited Love waves much more efficiently than did the explosions, with the difference in excitation increasing with increasing period. We conclude that this difference could be useful in discrimination of the two source types, even for relatively low magnitudes, e.g., near  $m_b = 4.4$ . We also conclude that the process of tectonic release was different for the explosions than for the earthquake, which was of comparable body wave magnitude. This strengthens our prior conclusion

that any tectonic effects are due to stress relaxation  
around the explosion-generated failure zone.

#### ACKNOWLEDGMENTS

This research was supported by the Advanced Research Projects Agency, Nuclear Monitoring Research Office, under Project VELA UNIFORM, and by the Air Force Office Scientific Research, Office of Aerospace Research, under contract number 70-1954, and was accomplished under technical direction of the Air Force Technical Applications Center under contract (F44620-69-C-0067). Once again we have been fortunate in having the able assistance of J. W. Lambert in performing the data processing and theoretical calculations.

#### REFERENCES

- Aki, K., Reasenburg, P., De Fazio, T., and Tsai, Y.B., 1969, Near-field and far-field seismic evidence for triggering of an earthquake by the Benham explosion: Bull. Seismol. Soc. Am., v. 59, p. 2197-2208.
- Alexander, S.S., 1963, Surface wave propagation in the western United States, Ph.D. Thesis, California Institute of Technology, Pasadena, California.
- Archambeau, C.B., Bradford, J.C., Broome, P.W., Dean, W.C., Flinn, E.A., and Sax, R.L., 1965, Data processing techniques for the detection and interpretation of teleseismic signals: Proc. IEEE, v. 53, p. 1860-1884.
- Archambeau, C.B. and Flinn, E.A., 1965, Automated analysis of seismic radiation for source characteristics: Proc. IEEE, v. 53, p. 1876-1884.
- Archambeau, C.B., 1968, General theory of elastodynamic source fields: Rev. Geophys., v. 6, p. 241-288.
- Archambeau, C.B., Flinn, E.A. and Lambert, D.G., 1969, Fine structure of the upper mantle: J. Geophys. Res., v. 74, p. 5825-5866.
- Archambeau, C.B. and Sammis, C., 1970, Seismic radiation from explosions in prestressed media and the measurement of tectonic stress in the earth: Rev. Geophys., v. 8, p. 473-499.
- Archambeau, C.B., 1971, The theory of stress wave radiation from explosions in prestressed media, submitted to Geophys. J., Roy. Astr. Soc.

REFERENCES (Cont'd.)

- Archambeau, C.B. and Minster, B., 1971, Representation theorems in prestressed elastic media with moving boundaries, in preparation.
- Ben-Menahem, A. and Harkrider, D.G., 1964, Radiation patterns of seismic surface waves from buried dipolar point sources in a flat stratified earth: *J. Geophys. Res.*, v. 69, p. 2605-2620.
- Eaton, J.P., 1963, Crustal structure from San Francisco, California, to Eureka, Nevada from seismic refraction measurements: *J. Geophys. Res.*, v. 68, p. 5789-5806.
- Evernden, J.F., 1970, ARPA symposium on seismic discrimination, opening presentation, Woods Hole, Massachusetts, v. 1, p. 1-13.
- Harkrider, D.G., 1964, Surface waves in multilayered elastic media: I. Rayleigh and Love waves from buried sources in a multilayered elastic half-space: *Bull. Seism. Soc. Amer.*, v. 54, p. 627-679.
- Harkrider, D.G., 1970, Surface waves in multilayered elastic media: Part II. Higher mode spectra and spectral ratios from point sources in phase layered earth models, *Bull. Seism. Soc. Amer.*, v. 60, p. 1937-1987.
- Press, F. and Archambeau, C.B., 1962, Release of tectonic strain of underground nuclear explosions: *J. Geophys. Res.*, v. 67, p. 337-343.

REFERENCES (Cont'd.)

- Rader, C. and Gold, B. 1969, Digital signal processing: New York, McGraw-Hill Book Co.
- Tsai, Y.B. and Aki, K., 1971, Amplitude spectra of surface waves from small earthquakes and underground nuclear explosions: *J. Geophys. Res.*, v. 76, p. 3440-3952.
- Toksöz, M.N., Harkrider, D.G. and Ben-Menahem, A., 1965, Determination of source parameters by amplitude equalization of seismic surface waves: Part 2. Release of tectonic strain by underground nuclear explosions and mechanisms of earthquakes: *J. Geophys. Res.*, v. 70, p. 907-922.

TABLE I

Description of data samples used

<u>Name</u>	<u>Date</u>	<u>m<sub>b</sub></u>	<u>Medium</u>	<u>Location</u>	<u>Origin Time (GMT)</u>	<u>Coordinates</u>
BILBY	13 Sep 63	5.8	Tuff	NTS	17 00 00.1	37 08 58 N 116 01 18 W
SHOAL	26 Oct 63	4.9	Granite	Sand Springs Ranges, Nev.	17 00 00.1	39 12 01 N 118 22 49 W
FALLON EARTHQUAKE	20 Jul 62	4.4	h = 15 km	Churchill City, Nevada	09 02 08.5	39 59 N 118 13 W

TABLE II

Source Parameters for Best Fit to Surface Wave Radiation Patterns

Equivalent fault type (double couple)	BILBY Right Lateral	SHOAL Right Lateral	Fallon Earthquake Right Lateral
Strike	N 342° E	N 353° E	N 10° E
Dip	90°	90°	82° E
Slip angle	0	0	16°
F	0.5	0.58	--



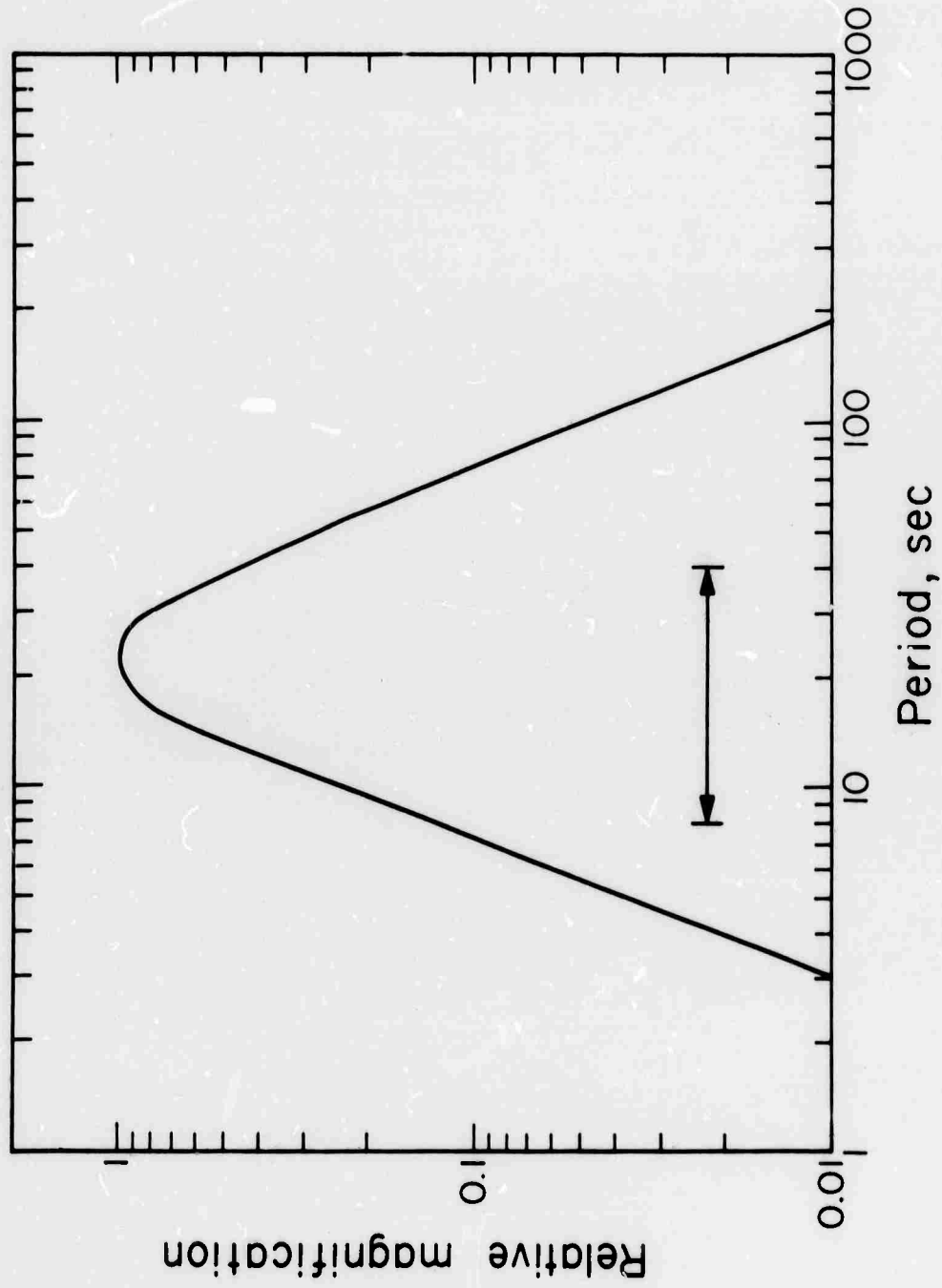


Figure 2. Long-period LRSM seismometer amplitude response curve. The indicated period range 8-40 second is the band within which good signal power was observed for the events studied.

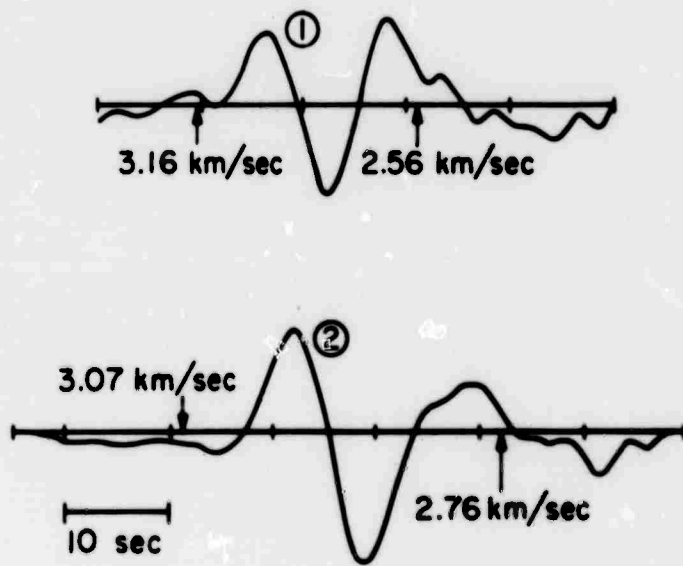
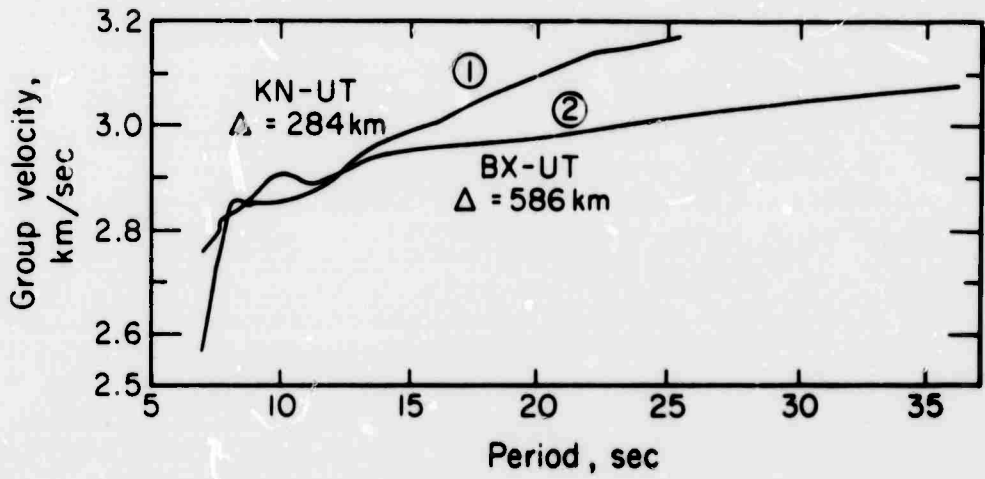


Figure 3. Samples of surface wave signals and the associated group velocity dispersion obtained from these signals using narrow band filtering methods.

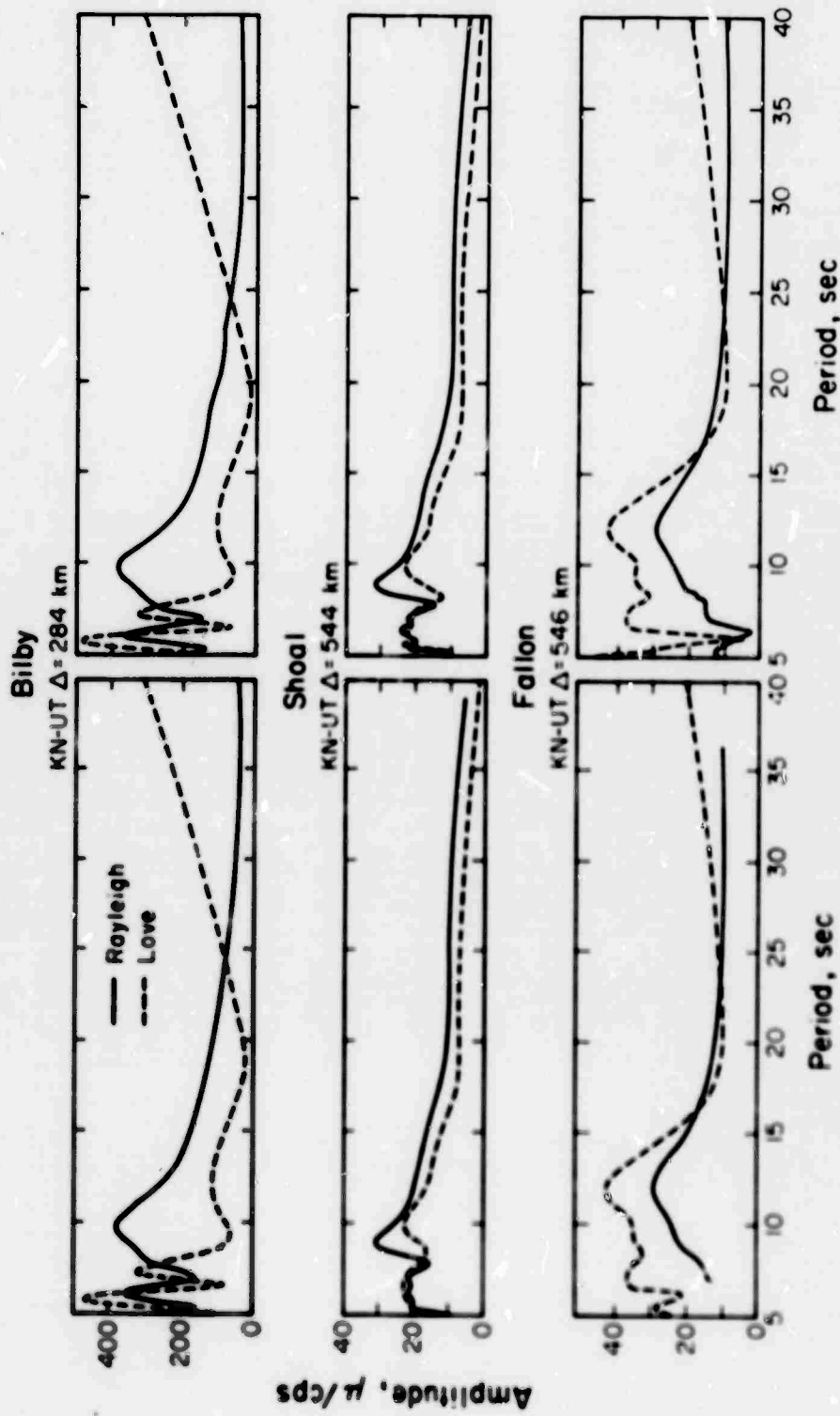
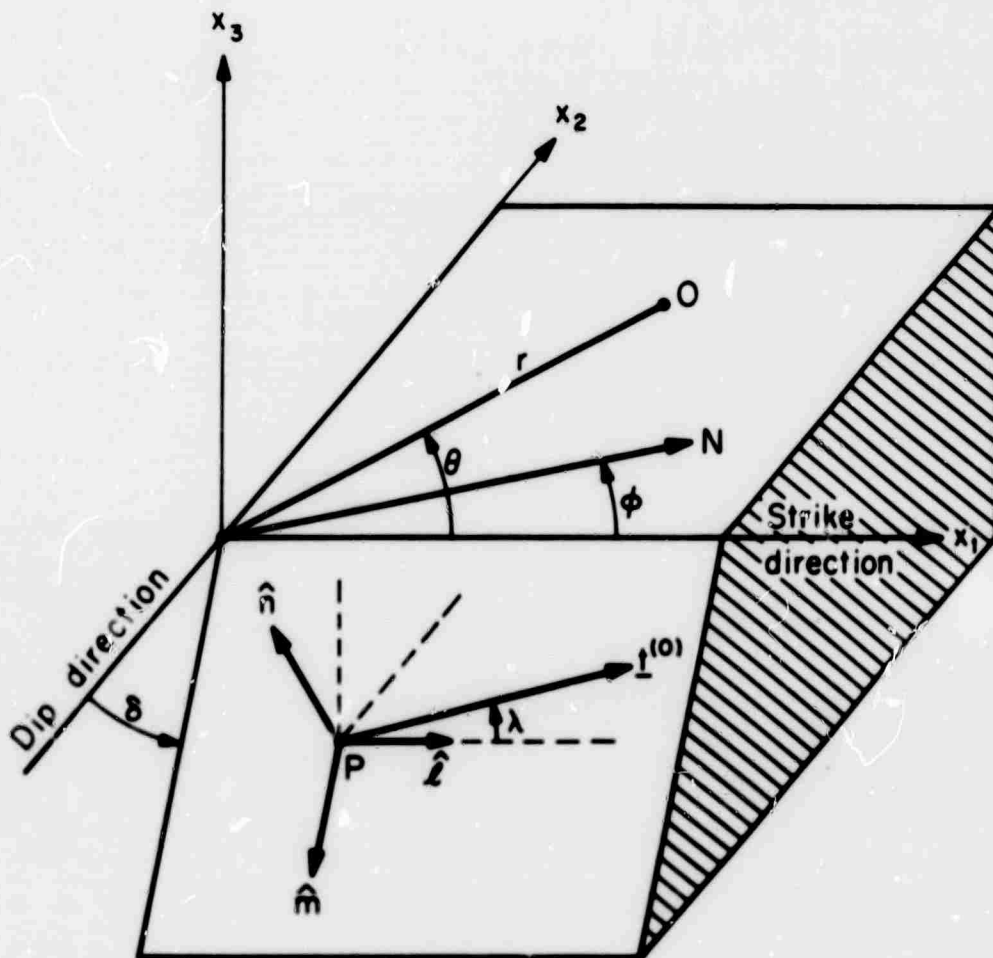


Figure 4. Samples of surface wave spectra from the three events studied. The signal sample and the group velocity for the BILBY Rayleigh spectra are shown in Figure 3. Fourier spectra of the signals are shown on the left and the group spectra obtained by narrow filtering on the right.



$\delta$  = Dip angle

$\phi$  = Strike angle

$\lambda$  = Slip angle

$\theta$  = Azimuth angle

$\hat{n}$  = Surface normal

$\hat{m}, \hat{l}$  = Orthogonal vectors  
in plane of surface

$\underline{t}^{(0)}$  = Traction vector in  
plane of surface

Figure 5. Fault (or traction) plane geometry. The point (O) is an arbitrary point of observation, while the vector N is in the direction of geographic North.

Q.

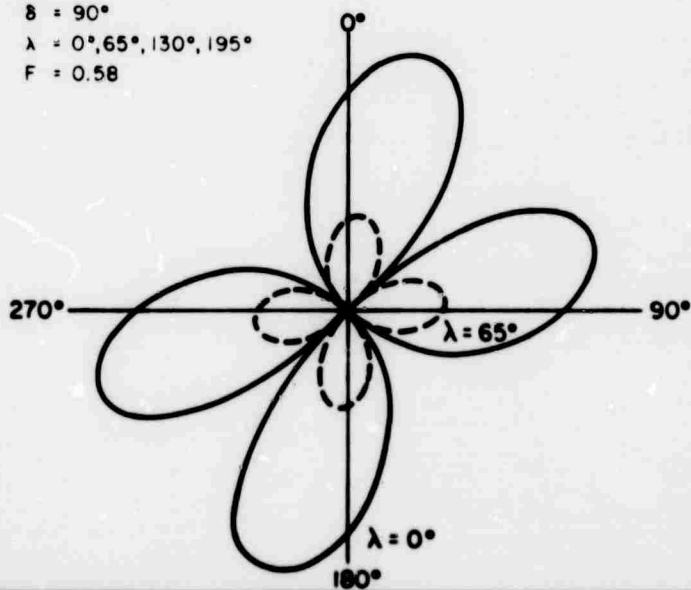
THEORETICAL LOVE TO RAYLEIGH  
WAVE AMPLITUDE RATIOS FOR AN  
EXPLOSION AND DOUBLE COUPLE  
AT 0 km DEPTH.

$$\phi = 0^\circ$$

$$\delta = 90^\circ$$

$$\lambda = 0^\circ, 65^\circ, 130^\circ, 195^\circ$$

$$F = 0.58$$



b.

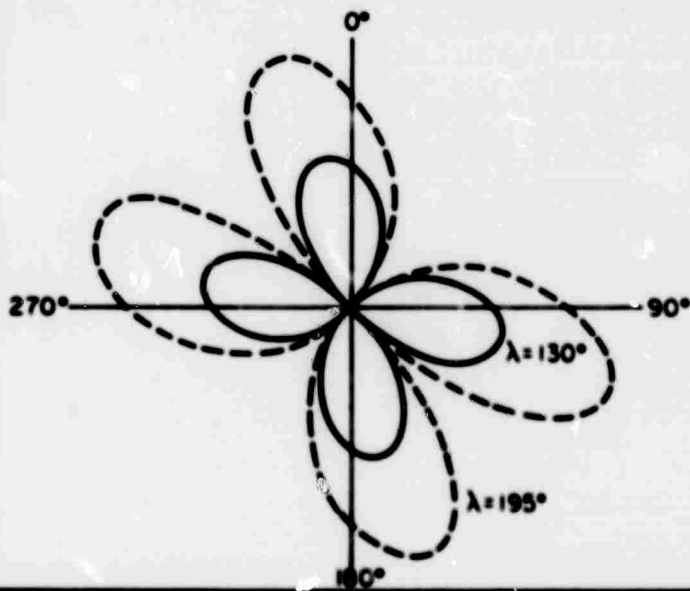


Figure 6. Variation of the Love to Rayleigh (L/R) wave ratio as a function of  $\lambda$ , the (double couple) "slip angle", for superposed monopole and quadrupole (double couple) components. The relative excitation of the quadrupole to monopole component is fixed at  $F = 0.58$  for all frequencies.

THEORETICAL LOVE TO RAYLEIGH  
WAVE AMPLITUDE RATIOS FOR AN  
EXPLOSION AND DOUBLE COUPLE  
AT 0 km DEPTH.

$\phi = 0^\circ$   
 $\delta = 30^\circ, 60^\circ, 90^\circ$   
 $\lambda = 0^\circ$   
 $F = 0.58$

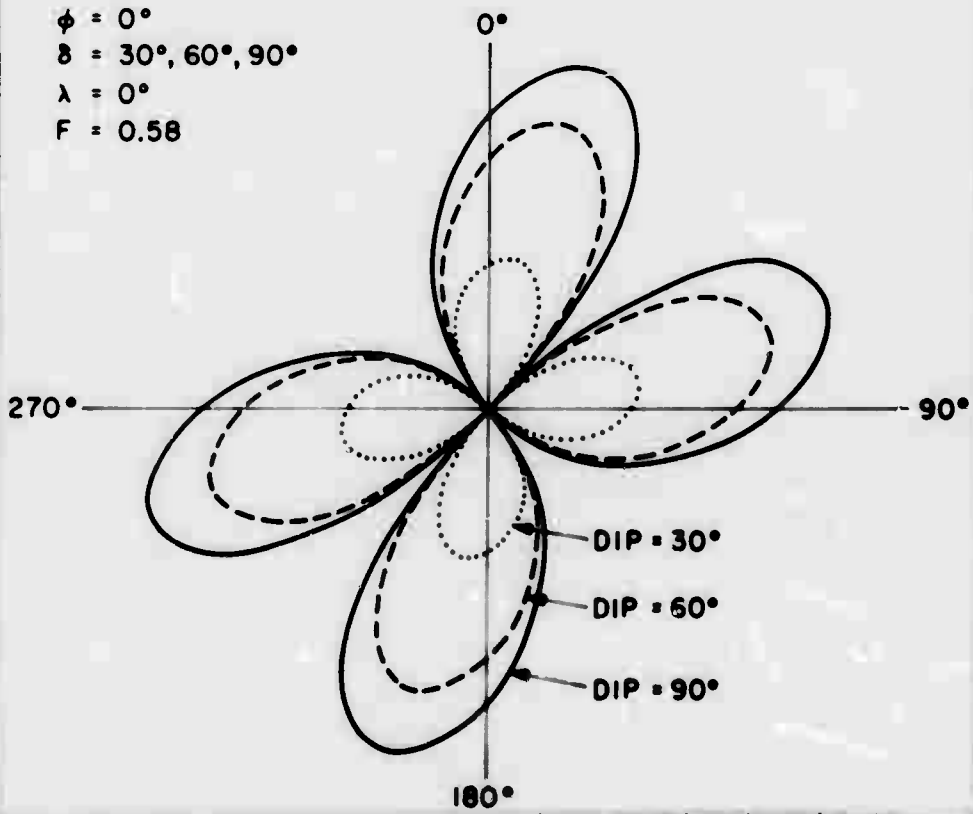


Figure 7. Variation of the Love to Rayleigh (L/R) wave ratio as a function of  $\delta$ , the (double couple) "dip angle", for superposed monopole and (double couple) quadrupole components. All other source parameters are fixed, as indicated.

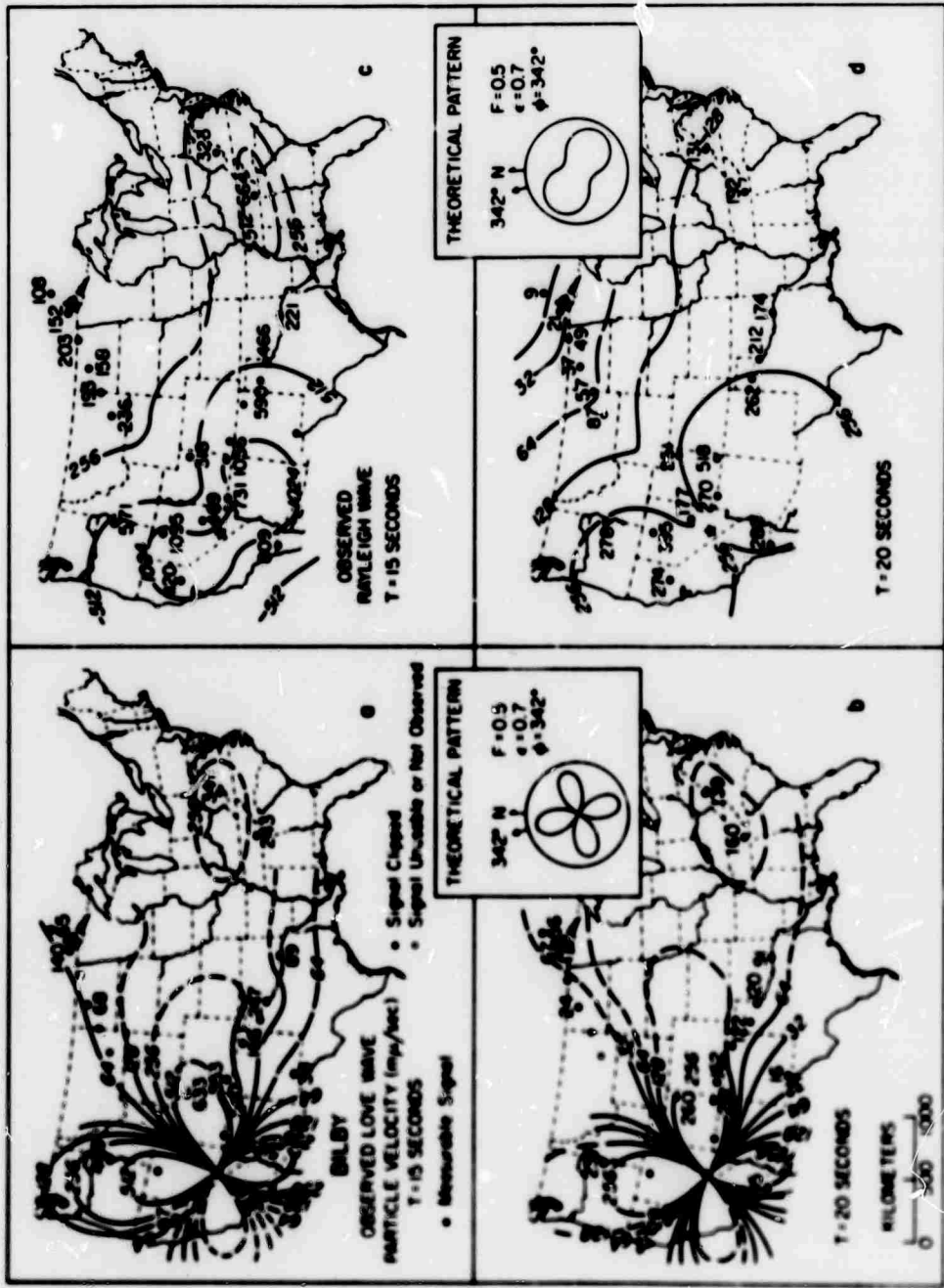


Figure 8. Radiation patterns of Love and Rayleigh waves from the underground explosion BILBY at periods of 15 and 20 seconds. The insets show the theoretical pattern shapes obtained as a fit to the observations using a superposed monopole and quadrupole point source with fixed relative excitation of quadrupole to monopole of  $F = 0.5$ , with the quadrupole "strike",  $\phi = 342^\circ$ . The point source equivalents are the same for both Love and Rayleigh waves. The factor  $\epsilon = 0.7$  is the particle orbit ellipticity factor for the Rayleigh waves and is dependent on the structure used in the theoretical calculations.

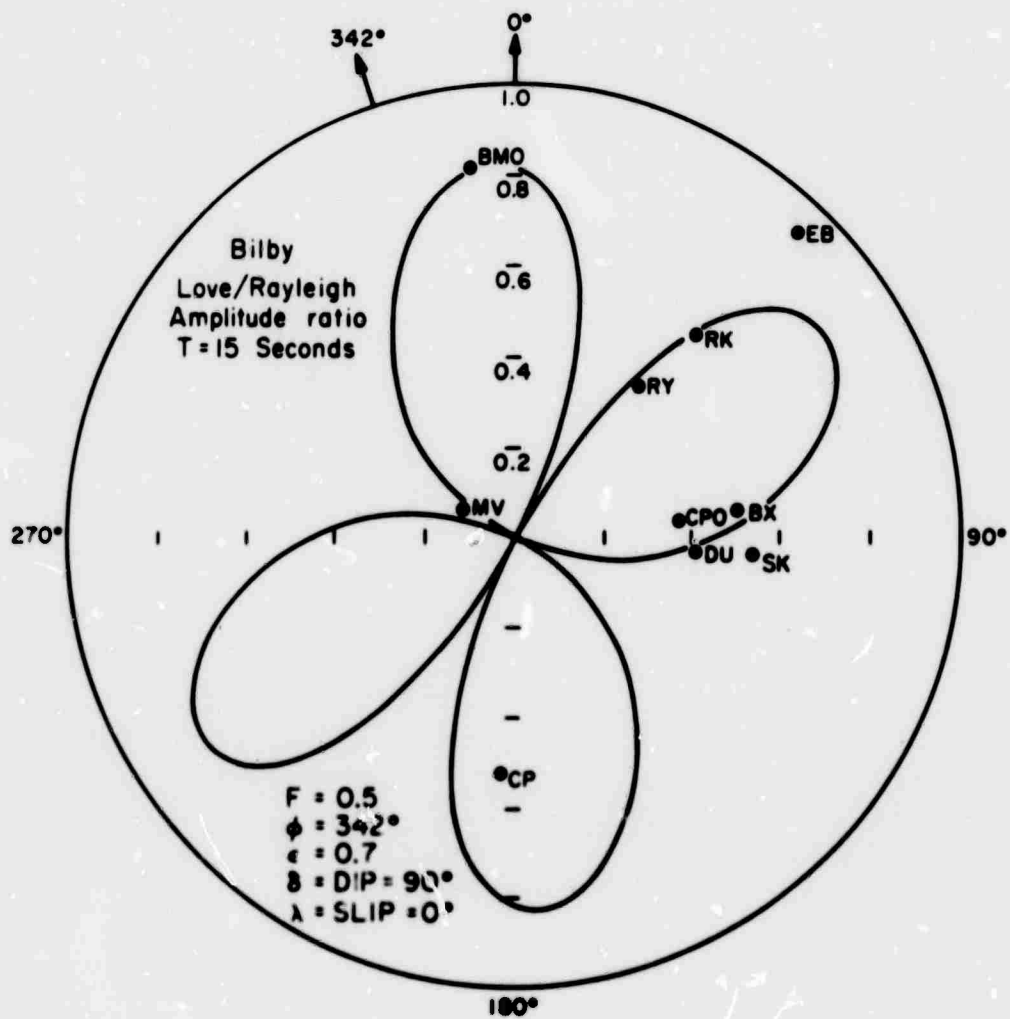


Figure 9. The theoretical Love to Rayleigh (L/R) wave ratio for BILBY, at T = 15 seconds, as a function of azimuth using the source parameters of Figure 8. The observed ratios at a number of stations with good signal to noise ratios for both Love and Rayleigh waves are shown at their appropriate azimuths. This also shows the nature of the L/R azimuth variation and that a single equivalent source fits both Love and Rayleigh wave radiation for this event.

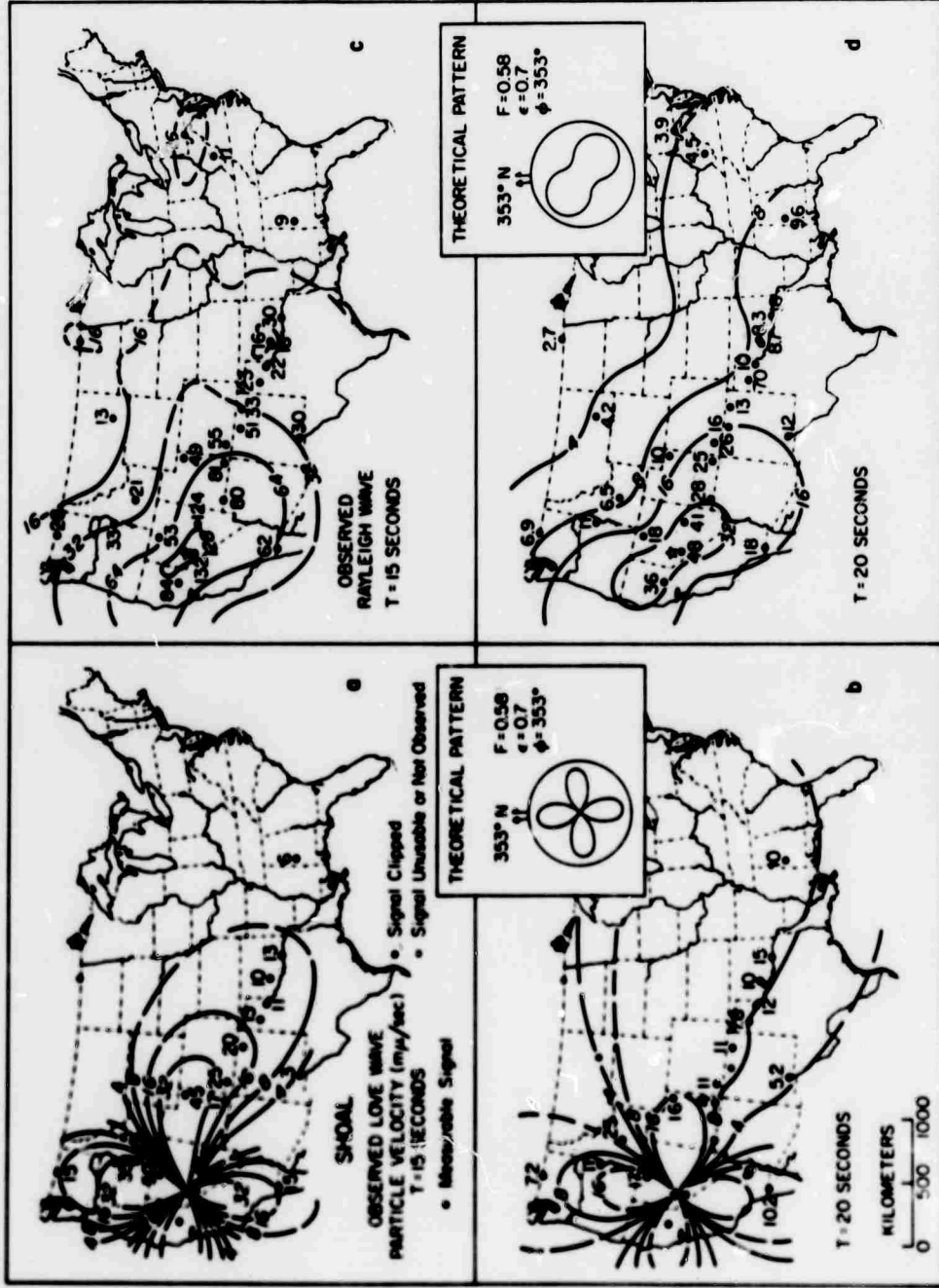


Figure 10. Radiation patterns of Love and Rayleigh waves from the underground explosion SHOAL at periods of 15 and 20 seconds. The insets show the theoretical patterns obtained as a fit to the observations using a superposed monopole and quadrupole point source with fixed relative excitation of quadrupole to monopole of  $F = 0.58$ , with the quadrupole "strike",  $\phi = 353^\circ$ . The point source equivalents are the same for both Love and Rayleigh waves.

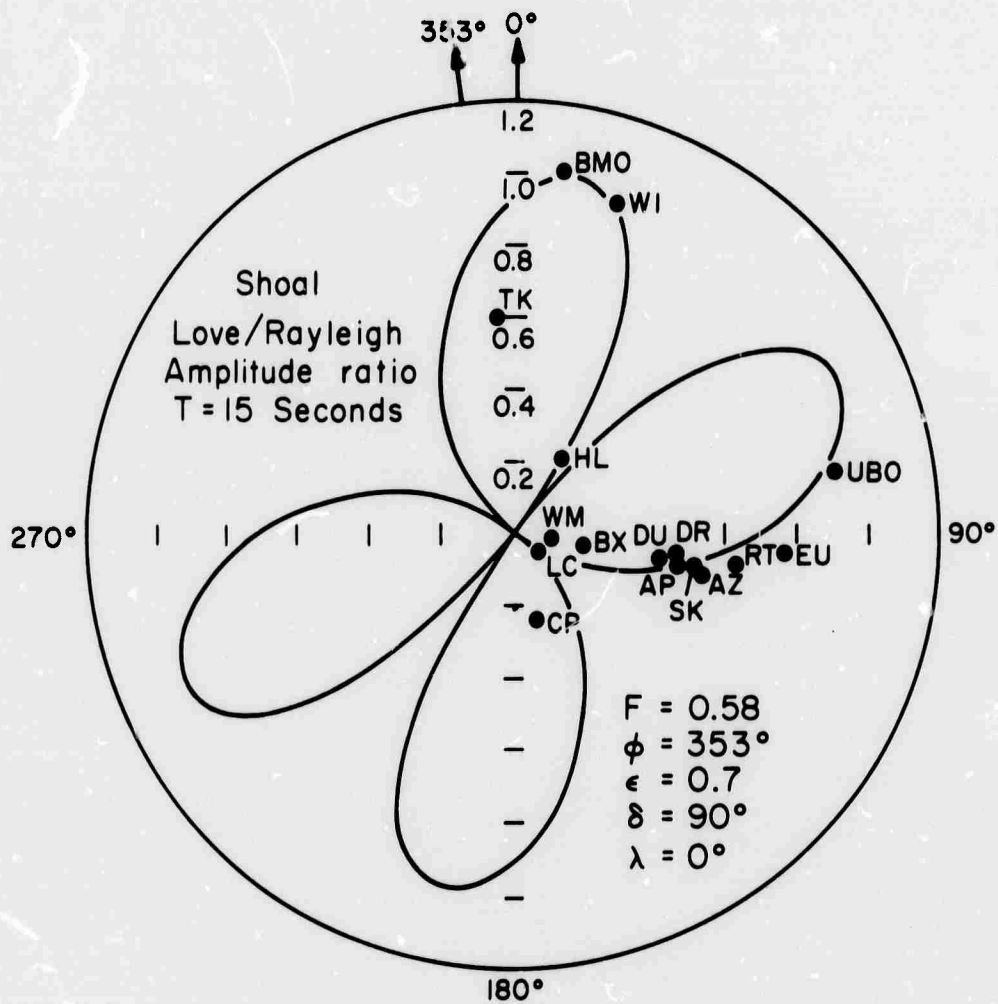


Figure 11. The theoretical Love to Rayleigh (L/R) wave ratio for SHOAL, at T = 15 seconds, as a function of azimuth using the source parameters of Figure 10. Observations at various azimuths where signal to noise ratios were high are indicated and identified by abbreviated station symbols. This also shows the nature of the L/R azimuth variation (which is nearly identical to that for BILBY) and that a single equivalent source fits both Love and Rayleigh wave radiation for this event.

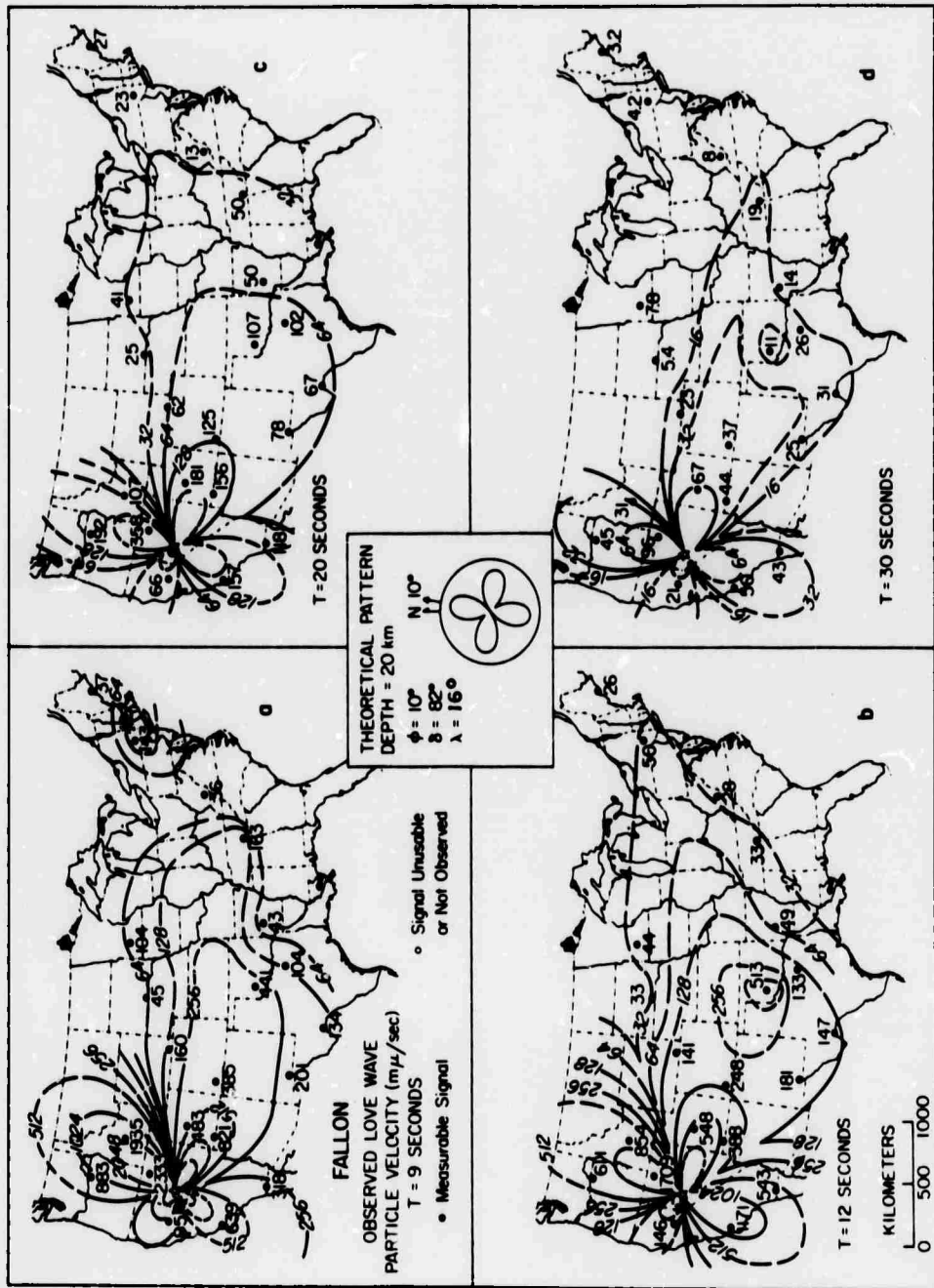


Figure 12. Radiation patterns for Love waves from the Fallon earthquake at periods of 9, 12, 20 and 30 seconds. The inset shows the theoretical pattern shape obtained as a fit using a point quadrupole (double couple) located and oriented as indicated. The orientation of the quadrupole is close to that obtained for SHOAL, indicating that the stress field orientation was similar for both. The data and contours for the field at  $T = 9$  seconds (a) show asymmetries in the near-source pattern indicating rupture propagation effects or perturbation in the pattern due to strong lateral variations in structure. These diminish with increasing period (b), (c), and (d), except for the point of observation in northern California. This anomaly may be due to the strong structural variation at the Sierra Nevada - Basin and Range boundary.

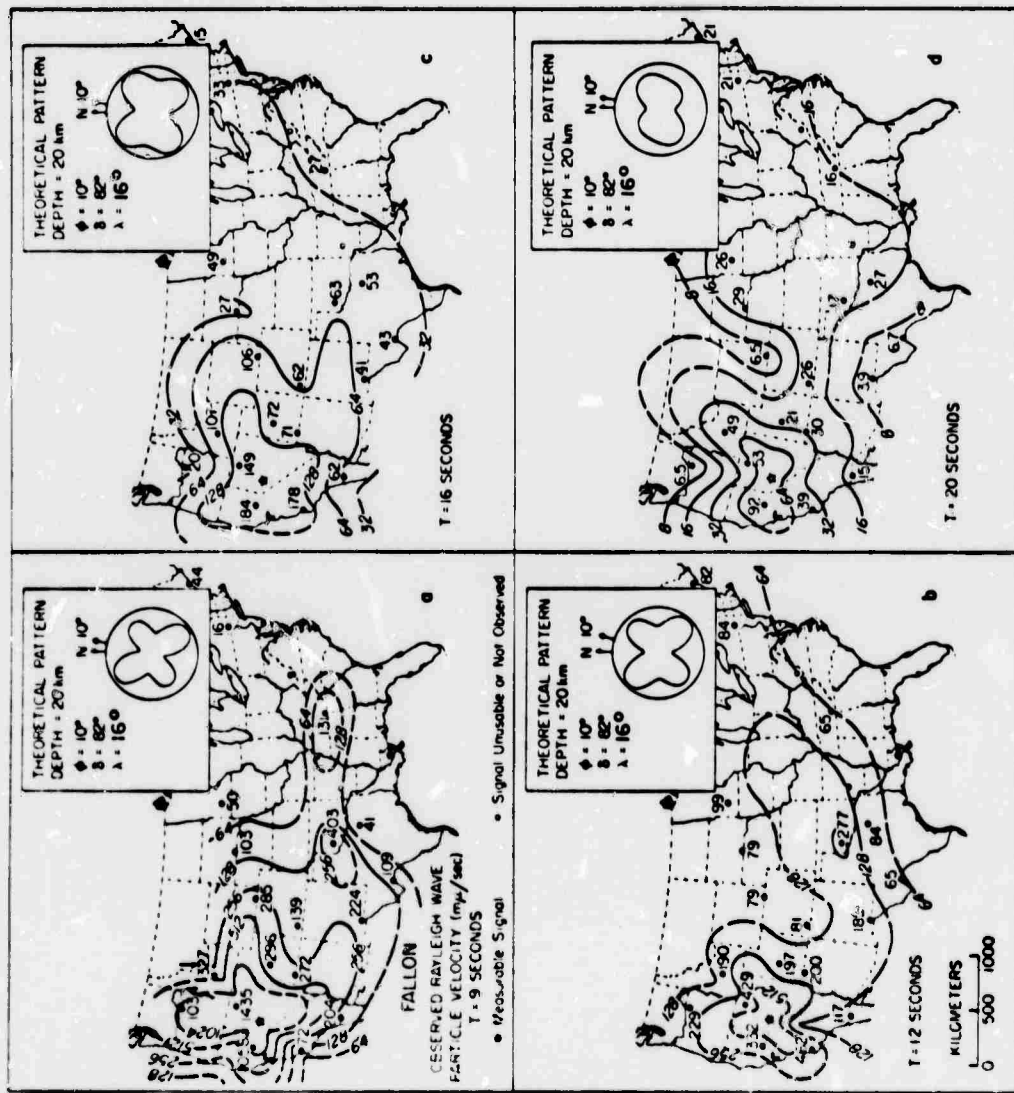


Figure 13. Radiation patterns for Rayleigh waves from the Fallon earthquake at periods of 9, 12, 16 and 20 seconds. The insets show theoretical patterns from the same point quadrupole source used to obtain the theoretical fits to the Love wave radiation patterns in Figure 12. The theoretical patterns for the Rayleigh waves change as a function of period, as opposed to the patterns for Love waves, due to the medium layering. This is a medium effect and should not be confused with any pattern shape change due to the intrinsic properties of the source itself. As was the case for Love waves, there appears to be evidence of rupture propagation effects in the asymmetry of the pattern at short periods ( $T = 9$  seconds in particular).

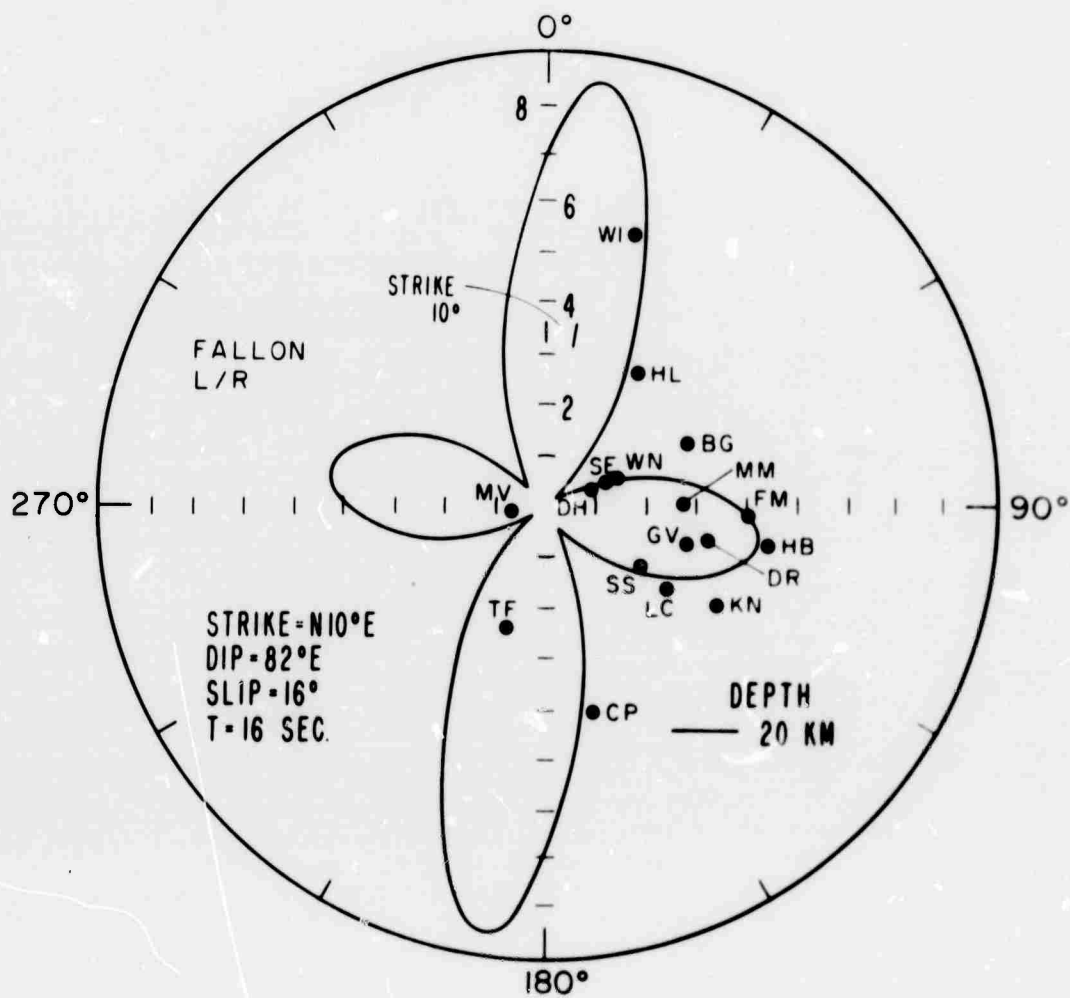


Figure 14. The theoretical Love to Rayleigh (L/R) wave ratio for Fallon, at  $T = 16$  seconds, as a function of azimuth using the source parameters obtained for the results shown in Figures 12 and 13. Observations at various azimuths where the signal to noise ratios were high are indicated and identified by abbreviated station symbols. This shows the nature of the L/R azimuth variation for an earthquake in the same environment as the comparable explosion: SHOAL (see Figure 11). The L/R ratio for this event is much larger than that for the explosion at all comparable azimuths, except along nodal lines.

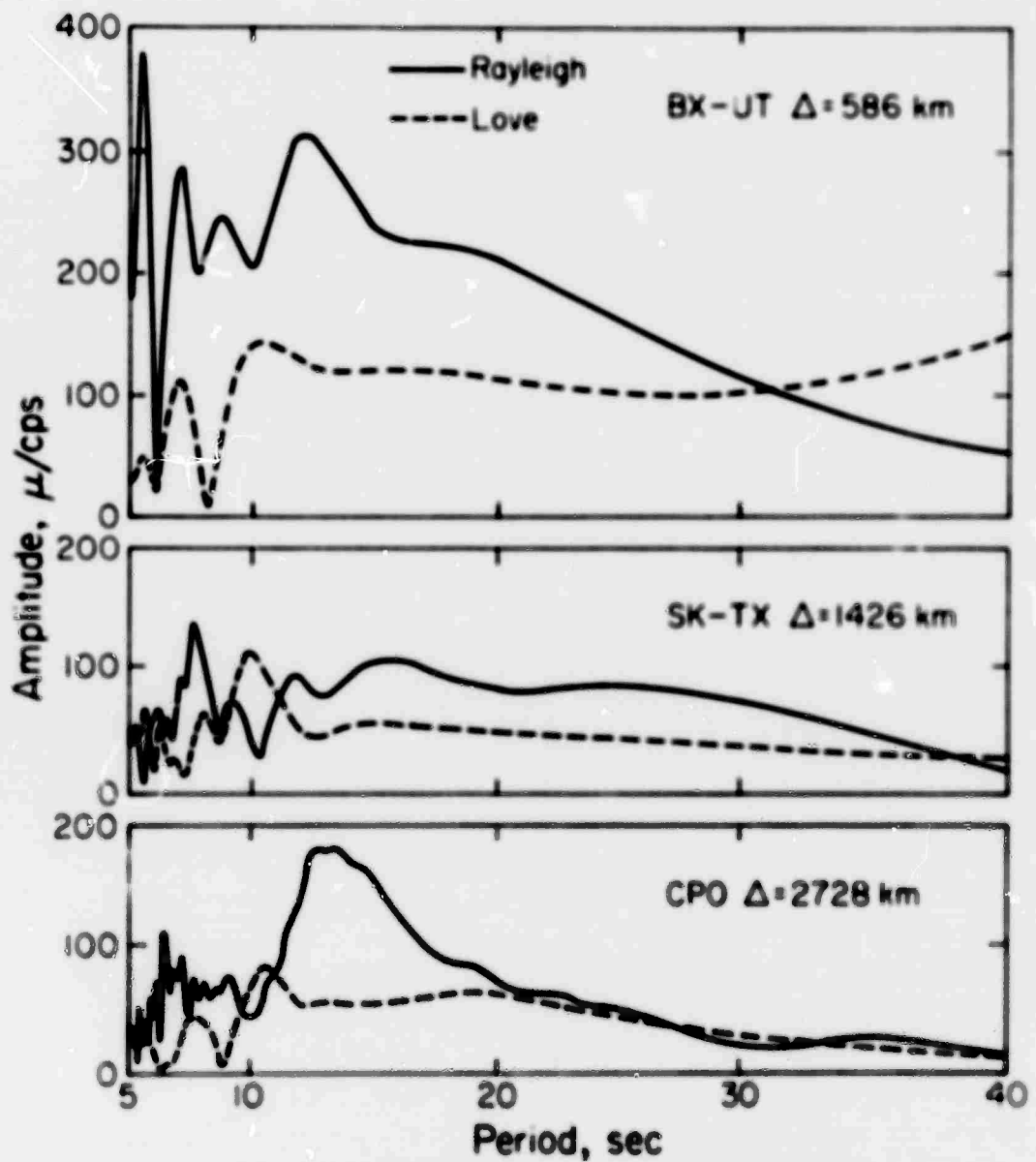


Figure 15. Surface wave spectra at 3 distances for the BILBY event. The points of observation are at approximately the same azimuth from the source. Note that the Rayleigh wave excitation is generally higher than the Love wave excitation.

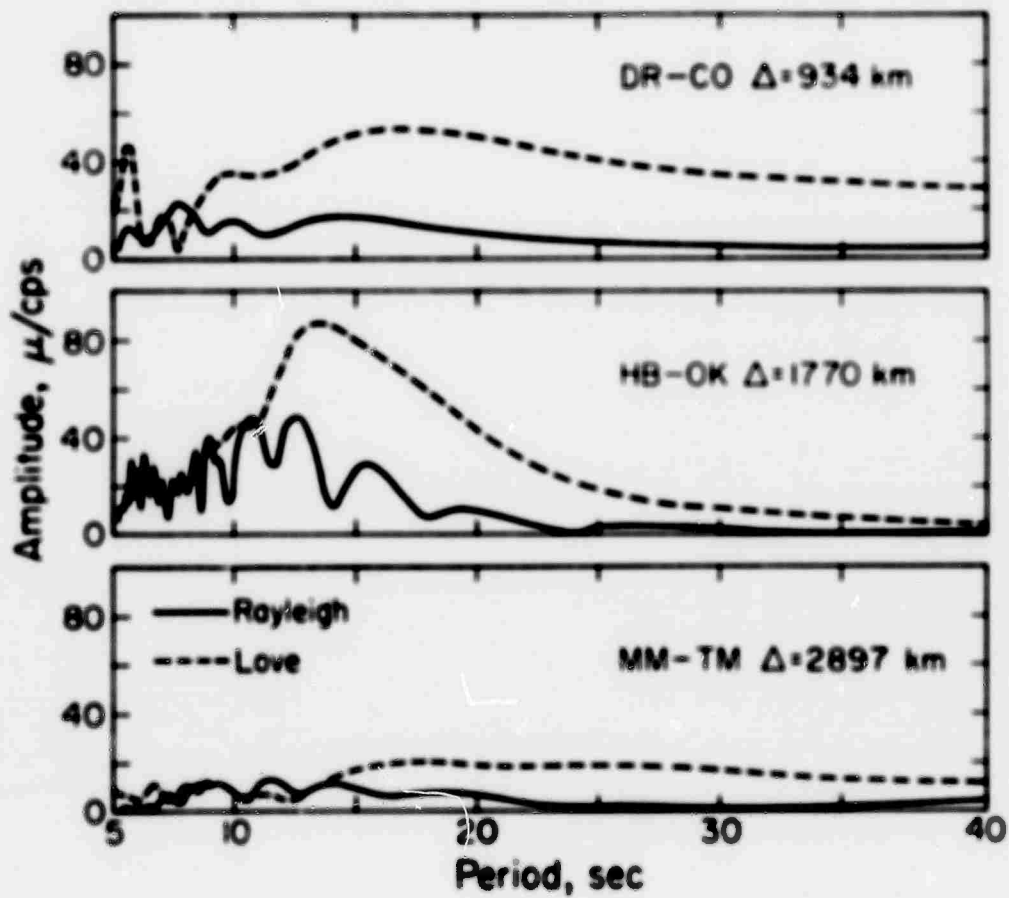


Figure 16. Surface wave spectra at 3 distances for the Fallon event. The points of observation are at approximately the same azimuth from the source. Note that the Love wave excitation is generally greater than the Rayleigh wave excitation.

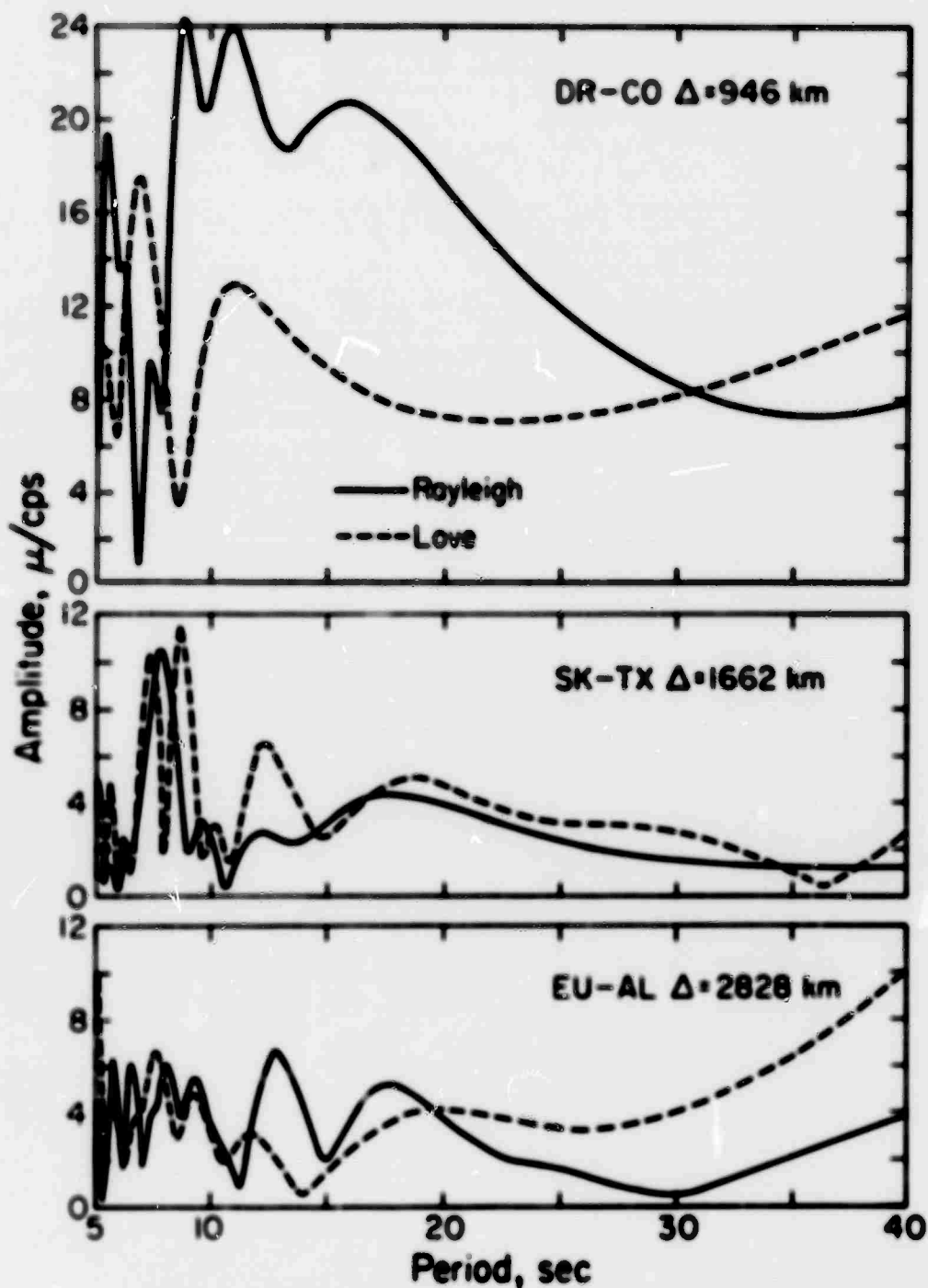


Figure 17. Surface wave spectra at 3 distances for the SHOAL event. The points of observation are at approximately the same azimuth from the source. The Love and Rayleigh excitation is of roughly the same order, although at the nearest (and most reliable) station the Rayleigh wave excitation is generally greater over the reliable period range.

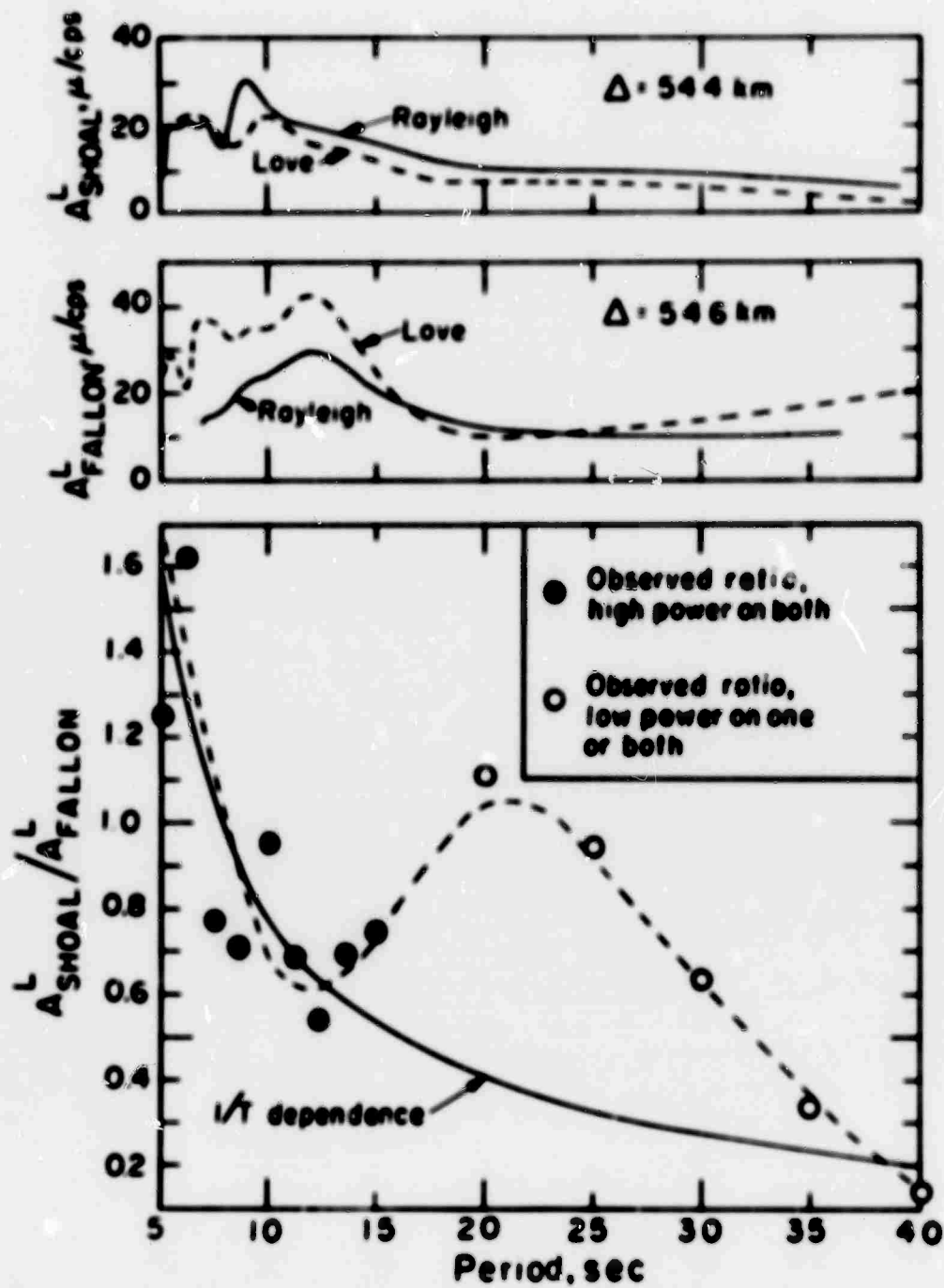


Figure 18. Love wave spectra and spectral ratios for the SHOAL and Fallon events. The upper two graphs show the Love wave spectra for the individual events with the Rayleigh wave spectra given for comparison. Both spectra are individually normalized to unity at the maximum power point and the resulting normalized ratio of SHOAL to Fallon Love wave spectral density is plotted. The sampled spectral ratio is shown by the data points, the dotted curve is a smoothed fit to these sample points and the solid curve a  $1/T$  curve given for comparison.

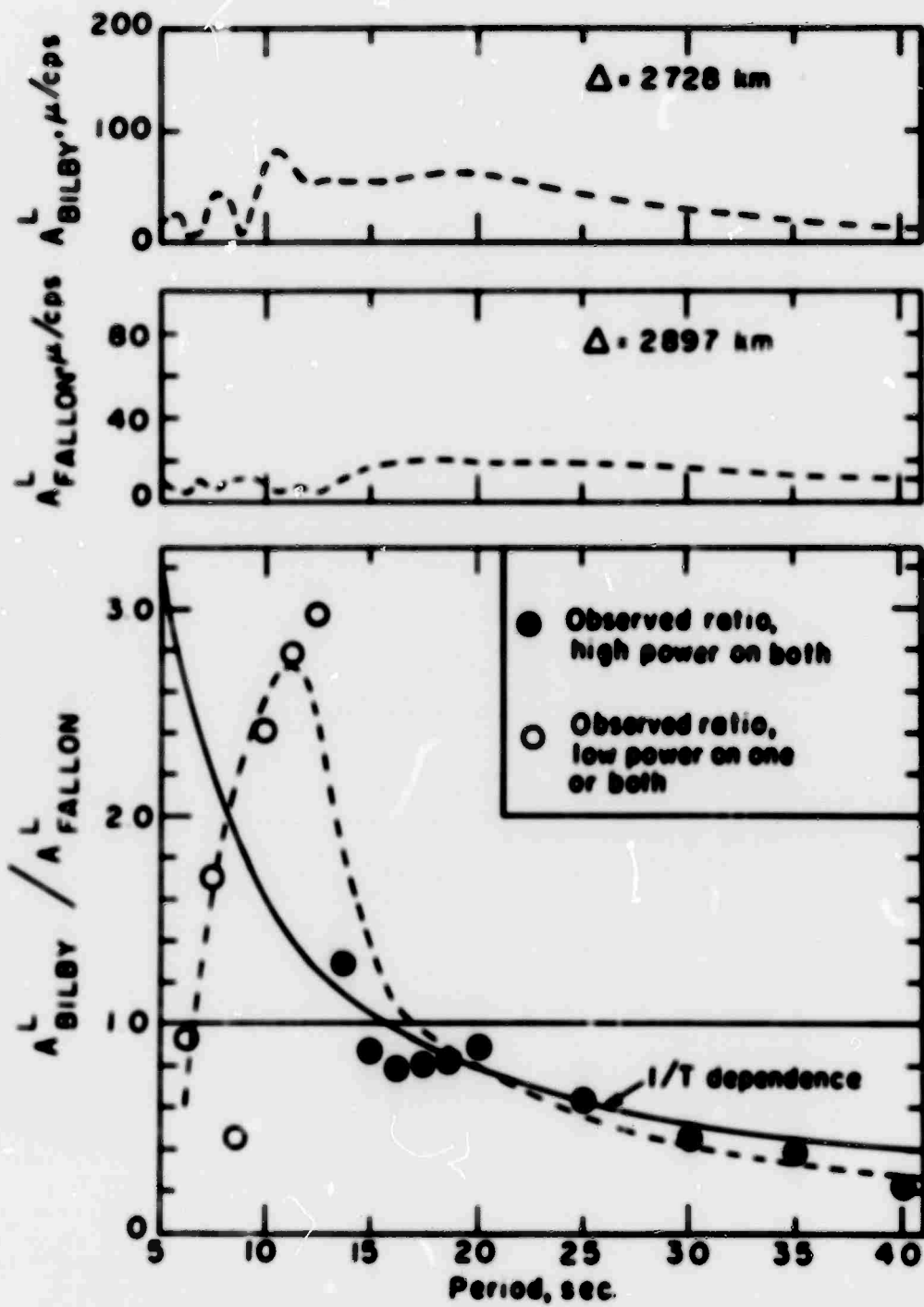
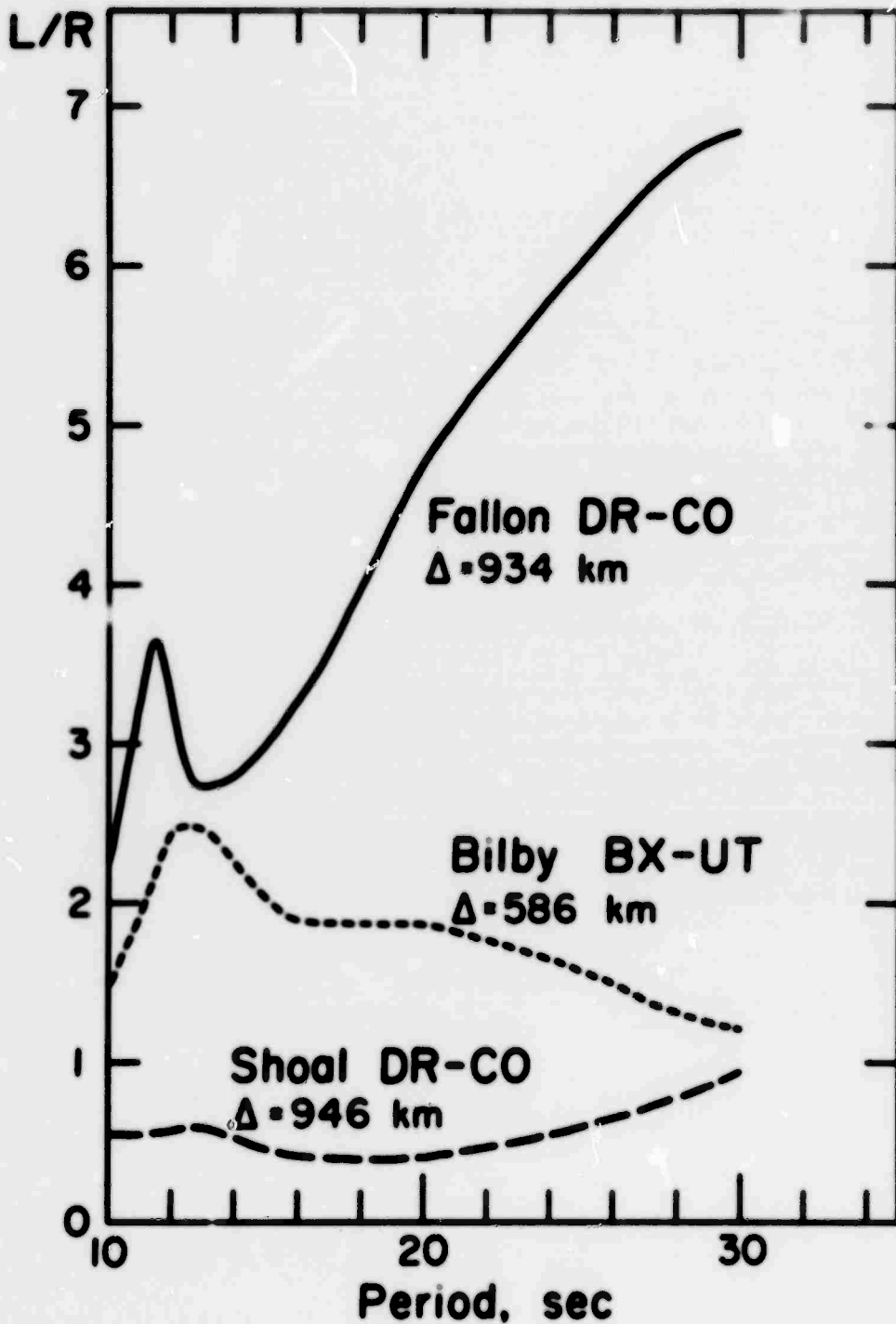


Figure 19. Love wave spectra and spectral ratios for the BILBY and Fallon events. The upper two graphs show the Love wave spectra for the two events and the lower graph the normalized spectral ratio as described in Figure 18.



**Figure 20.** The variation of  $L/R$  versus period for the BILBY and SHOAL explosions and the Fallon earthquake, in the distance range near 800 km. The  $L/R$  for the earthquake is larger than 2 and increases with increasing period, while  $L/R$  for the earthquake is larger than 2 and increases with increasing period, while  $L/R$  for the explosions is between 1 and 2 and remains nearly constant with increasing period. This difference in behavior is a consequence of the much larger source dimension associated with the earthquake.

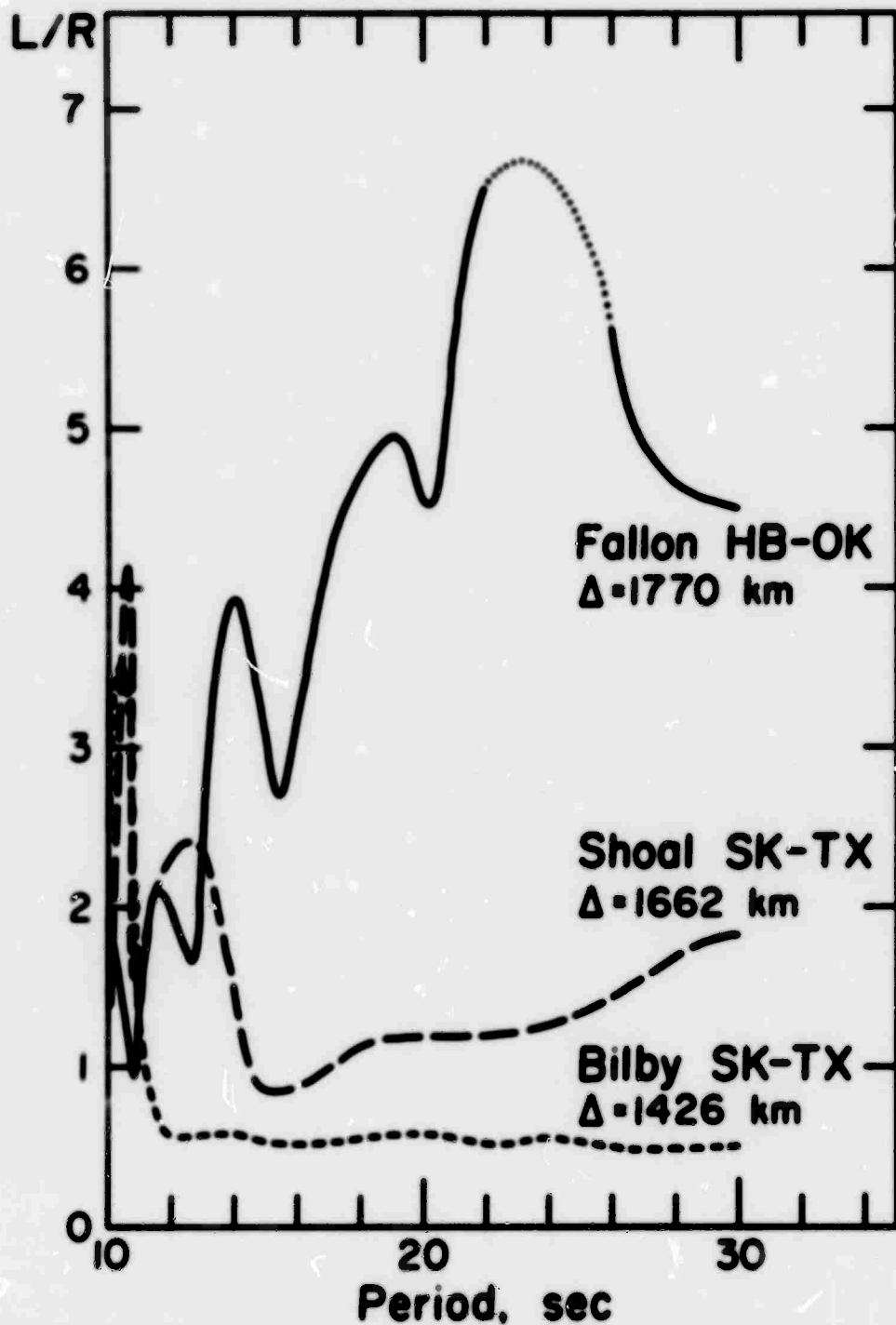


Figure 21. The variation of L/R versus period for the BILBY and SHOAL explosions and the Fallon earthquake, in the distance range near 1600 km. The L/R for the earthquake is again considerably larger than that for the explosions and increases with increasing period at this larger distance range, as expected. Note, however, that the details in the variation of L/R period, i.e., local maxima and minima, are considerably different than in Figure 20 and that the separation in the L/R is obscured at the short period end of the range.

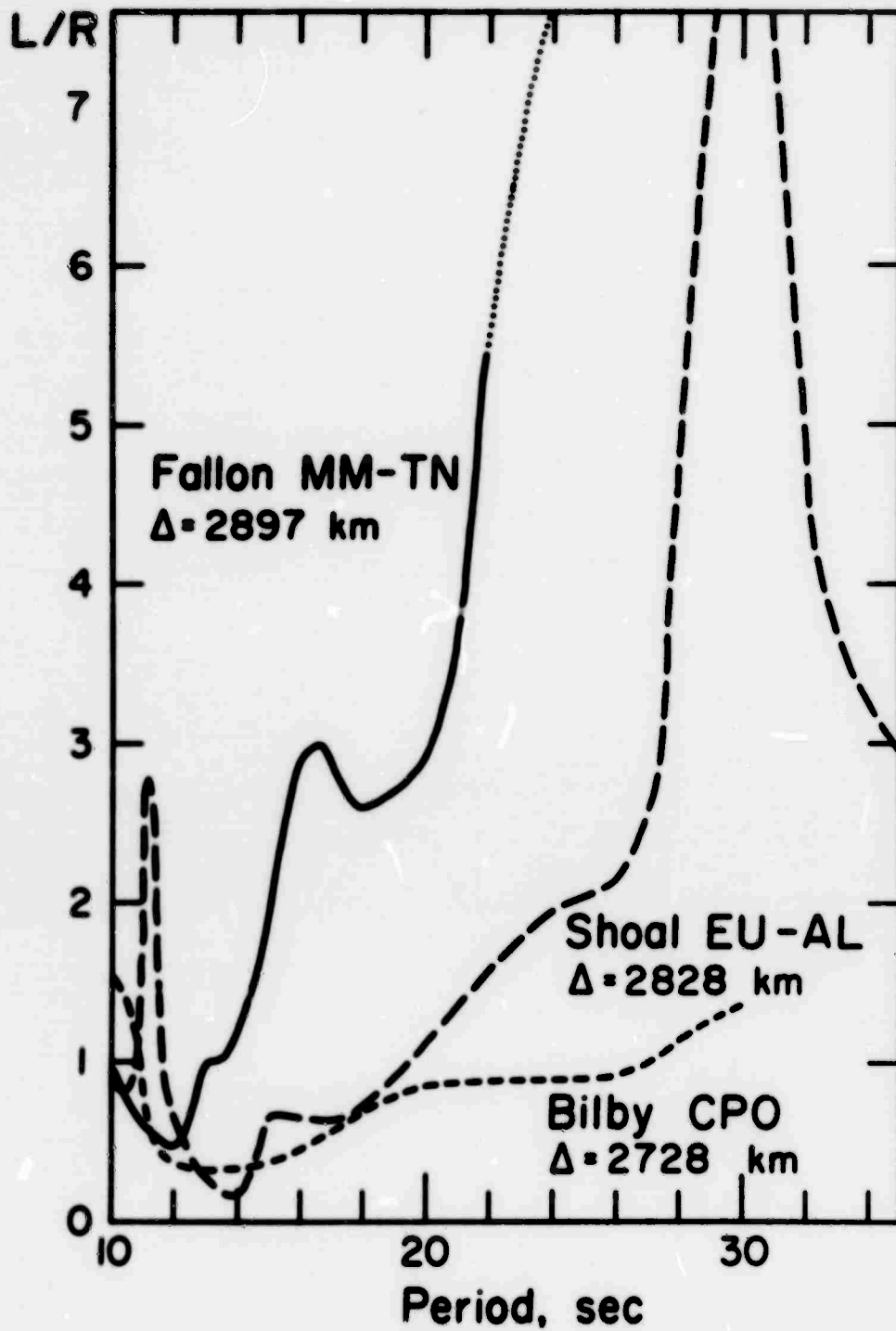


Figure 22. The variation of L/R versus period for the BILBY and SHOAL explosions and the Fallon earthquake, in the distance range near 2800 km. At large distances the L/R separation between the earthquake and the explosions is maintained at long periods. The peak in the spectral ratio for Shoal at 30 seconds is probably due to a path effect.

APPENDIX I

A-1

## THEORETICAL BACKGROUND

We begin with the stress relaxation source described by Archambeau (1968) and Archambeau and Minster (1971). First we present briefly the analytical nature of this field representation, and show that for the purposes of the present study it is sufficient to replace the actual source by an equivalent point source whose primary contribution to the far-field radiation is a quadrupole term at the long-wavelength end of the spectrum. We are thus able in this approximation to make use of the point-source models described by Ben-Menahem and Harkrider (1964), and in particular to use Harkrider's computer program to calculate a theoretical fit to our observations of radiation patterns.

For the explosion sources studied here, we adopt the hypothesis that the observed anomalous shear wave energy is due to tectonic effects. This idea has been considered in some detail by Press and Archambeau (1962), Toksöz et al. (1965), Archambeau and Sammis (1970), and Tsai and Aki (1971), among others. At the present stage we do not assume any specific model for the process of tectonic release, i.e., we do not choose beforehand among the following possibilities: (1) all the tectonic release is due to the creation of a simple, nearly spherical, shatter or failure zone caused by the shock wave from the explosion; (2) all or most of the tectonic energy

A-2

release is due to the triggering of rupturing which results in the creation of lineal failure zones larger than the shatter zone. Instead of adopting either of these hypotheses, we present here a theory which covers both cases, and study the observed spectral data from the explosions in order to attempt to determine whether or not tectonic release actually contributes to the radiation field, and if so, which of these "geometrical" mechanisms is responsible.

As far as the direct contribution to the radiation field from explosion-generated shock waves is concerned, it will be assumed as a working hypothesis that the field is adequately represented by a monopole contribution. Because of inhomogeneities and anisotropy in the source region, which will affect the conversion of the shock waves to elastic waves, there will undoubtedly be higher-order multipole contributions, but it is reasonable to consider these as second order compared to the monopole term (Toksöz et al., 1965), and also of second order compared to the hypothesized tectonic effects. However, one of the purposes of this study is to assess the relative importance of any tectonic effects compared to the non-monopole contributions to the far-field radiation from the explosive sources. Consequently, although we adopt a reasonable working hypothesis in order to have a basis for the development of a theoretical framework, we do not exclude

other possibilities from our interpretive considerations.

Stress relaxation effects for both explosions and earthquakes have been considered in some detail by Archanbeau (1968, 1971) and here we need merely summarize these briefly. The treatment is based on an initial-value formulation, with the medium assumed to be in a prestressed equilibrium state, so that upon creation of a failure zone the solid medium relaxes to a new equilibrium state and a new state of stress. This is accomplished by radiation of energy away from the volume surrounding the failure zone, with a net reduction of potential (or strain) energy within this region; this process is naturally described as an initial-value problem. The energy release is, of course, due to the change in effective material properties in the failure zone, since afterward the medium will not be able to sustain the same stress, i.e., it cannot maintain the initial equilibrium.

We can treat such a problem quite simply in an unbounded medium, and then add to the result the solution to the homogeneous problem (no source terms or initial values) in order to satisfy specified conditions on boundaries within or surrounding the actual volume of interest.

The equations of motion for the infinite homogeneous, isotropic, perfectly elastic, prestressed solid medium, neglecting higher-order interactions with the prestress field,

A-34

can be reduced to the set of wave equations (Archanbeau, 1971):

$$\nabla^2 \chi_a - \frac{1}{v_a^2} \frac{\partial^2 \chi_a}{\partial t^2} = -4v_a q_a \quad ; \quad a = 1, 2, 3, 4 \quad (1)$$

where the four potentials  $\chi_a$ , representing the three components of rotation and the scalar dilatation (the scalar having index  $a = 4$ ) provide the displacement field via the relations:

$$\frac{\partial^2}{\partial t^2} u_i = v_c^2 \frac{\partial \chi_c}{\partial x_i} - 2v_k^2 \delta_{ijk} \frac{\partial}{\partial x_j} \chi_k \quad (2)$$

where the indices  $i, j, k$  run over the range 1, 2, 3 and  $\delta_{ijk}$  is the alternating tensor. Here we employ the usual summation convention;  $v_k$  is the shear velocity for each  $k = 1, 2, 3$ , while  $v_4$  is the compressional velocity.  $q_a$  in equation (1) represents any explicit body force (e.g., gravity or internally applied force loads). In the present problem we can represent the explosion itself by a distribution of forces over a surface within the medium, and we could use a delta function form for  $q_a$  to accomplish this representation.

The potentials  $\chi_a$  are dynamic field potentials defined (or measured) relative to the final equilibrium state of the medium. The prestress does not appear explicitly in these equations, but it will appear as a generalized initial value for these potentials since they have non-zero values appropriate

to the initial state of stress at the onset of the failure process and will eventually assume final (zero) values appropriate to a state of stress in equilibrium with the completed failure zone. The change in the potentials at a given stage of the rupture zone configuration is given by Archanbeau (1971) as:

$$\nabla^2 \chi_a^* = 0 \quad (3)$$

and thus the change in the  $\chi_a$  for a change in material properties due to failure is always a harmonic function.

A Green's function solution for equation (1) provides a convenient method of introducing the initial values of  $\chi_a$ , and shows the effects of other source terms, as well as interactions between the field and boundaries within the medium.

We have (e.g., Archanbeau, 1971):

$$\begin{aligned} \chi_a(\underline{r}, t) = & \int_0^{t^+} dt_0 \int_V G_0(\underline{r}, t; \underline{r}_0, t_0) \varphi_a(\underline{r}_0, t_0) d\underline{r}_0 \\ & + \frac{1}{4\pi} \int_0^{t^+} dt_0 \oint_S \left\{ G_0 [\nabla_0 \chi_a] - [\chi_a] \nabla_0 G_0 \right\} \cdot \underline{n}_0 \\ & + \frac{1}{4\pi v^2} \int_0^{t^+} dt_0 \int_V \frac{\partial}{\partial t_0} \left\{ \chi_a \frac{\partial G_0}{\partial t_0} - G_0 \frac{\partial \chi_a}{\partial t_0} \right\} d\underline{r}_0 \end{aligned} \quad (4)$$

A-6

where, as previously noted, we will use the Green's function for an infinite space, given by:

$$\nabla_0^2 C_0 - \frac{1}{v_0^2} \frac{\partial^2}{\partial t_0^2} C_0 = 4\pi \delta(\underline{r}-\underline{r}_0) \delta(t-t_0)$$

The first term in (4) corresponds to the particular effects of body force terms or time-varying applied forces, and in considerations of tectonic effects per se these will be omitted from further attention. The second term will also be ignored for the present, since it represents the interaction of the field with boundaries, including the boundary enclosing the growing failure zone. Since the individual parts of the field, both due to the source and to boundary "scattering" effects, are additive, we can superpose the effects of the boundaries later, using a solution involving an eigenfunction expansion which is equivalent to the surface integral term. We are left only with the last term in the solution (4) which is thus seen to take into account the initial-value effects.

Now we consider the effect of introducing a shock-generated failure zone due to an explosion (for details of the development, see Archanbeau, 1971). We assume that the creation of this zone proceeds at a rate faster than any of the intrinsic wave velocities within the medium, and if we take the shape of the zone of failure to be spherical as a first approximation,

A-7

then we have in effect, an instantaneous creation of a shatter zone. In this case, denoting the last term in (4) as  $\chi_0^{(1)}(r, t)$ , we have:

$$\chi_0^{(1)}(\underline{r}, t) = \frac{1}{4\pi v_0^2} \int_0^{t^*} \frac{d}{dt_0} \left[ \int_V \left( \chi_0 \frac{\partial \dot{G}_i}{\partial t_0} - G_i \frac{\partial \chi_0}{\partial t_0} \right) d\underline{r}_0 \right] dt_0$$

with an initial state given by:

$$[\chi_0]_{t_0=R/v_R} = \chi_0^*(\underline{r}_0)$$

$$\left[ \frac{\partial \chi_0}{\partial t_0} \right]_{t_0=R/v_R} = 0$$

where  $R$  is the radius of the shatter zone and  $v_R$  is the rupture velocity, which we here take to be equal to the shock velocity for the medium. Thus the initial values are defined at the time of completion of the rupture, and relaxation proceeds from that time onward at a rate governed by the intrinsic velocities within the medium. We note that the initial value  $\chi_0^*$  is given by the solution of (3) along with continuity conditions on the rupture surface and a condition requiring  $\chi_0^*$  to approach the unperturbed initial value at large distances from the rupture zone. That is, we require a solution to the standard problem for a spherical inclusion in a stressed medium. Integrating over the source time variable

$t_0$  and taking account of the discontinuous nature of the integrand, we find:

$$x_0^{(2)}(\underline{x}, t) = -\frac{1}{4\pi v_0^2} \int_V x_0^* \left( \frac{\partial G_0}{\partial t_0} \right)_{t_0=t_0} dV_0 \quad (5)$$

Here  $x_0^*$  is a known harmonic function and  $G_0$  is the Green's function for the infinite-space problem. Thus we have an explicit volume integral to evaluate, which is a quite straightforward problem.

When the rupture velocity is less than the intrinsic velocity  $v_0$ , relaxation of stress occurs as the rupture volume increases or changes shape. This is the case for spontaneous failure and thus is appropriate for the earthquake source model.

If we view this process as a sequence of instantaneous sub-processes, each separated by an incremental time  $\delta t_0$ , we can add together solutions of the form (5) to get the effect of finite rupture velocity in the stressed medium. In the limit as  $\delta t_0$  approaches zero, this will yield the required solution (see Archanbeau, 1968 and 1971, for an expanded discussion). Thus, taking the rupture growth in

A-9

steps at  $t_{0k}$  times  $k = 1, 2, \dots$ , each growth increment being separated in time by  $\Delta t_0$ , we obtain by superposing solutions (5):

$$\chi_0^{(1)}(\underline{r}, t) = - \frac{1}{4\pi v_0^2} \sum_k \Delta t_0 \int_V \left( \frac{\delta \chi_0^*}{\delta t_0} \right) \left( \frac{\partial G}{\partial t_0} \right)_{t_{0k}} d\underline{r}_0$$

Here we have inserted  $\Delta t_0$  explicitly by multiplying and dividing (5) by the time increment. The quantity  $\delta \chi_0^*$  is seen to be

$$\delta \chi_0^* = \lim_{\epsilon \rightarrow 0} [\chi_0^*(t_{0k} - \epsilon) - \chi_0^*(t_{0k} + \epsilon)]$$

and this corresponds to the change in the equilibrium field due to the increment of rupture growth which occurs at time  $t_{0k}$ .

Now if we allow  $\Delta t_0$  to approach zero while simultaneously allowing the number of growth increments to approach infinity, the summation becomes an integral and the difference ratio  $\delta \chi_0^* / \Delta t_0$  becomes a partial derivative, and so we have:

$$\chi_0^{(1)}(\underline{r}, t) = \int_0^t U(t_0 - t_0) dt_0 \int_V \left( \frac{\partial \chi_0^*}{\partial t_0} \right) \left( \frac{\partial G}{\partial t_0} \right) d\underline{r}_0 \quad (6)$$

Here  $U(t_0 - t_0)$  is a unit step function and  $t_0$  is the time during which rupturing occurs. When  $t_0 > t_0$  this step function

A-16

vanishes; it is unity for  $t_0 < t_0$ , and thus it merely serves to define the time interval of the rupture process and hence the interval of integration over the source time  $t_0$ .

In both the forms (5) and (6), the solution for the field caused by the relaxation,  $\lambda_0^*$ , has the same meaning. In particular, it is the equilibrium field for the prestressed medium with an inclusion (the rupture zone). The nature of the inclusion, i.e., its shape, size, and so forth, is dependent on the "source" time  $t_0$ , since we allow the inclusion to change shape as a function of time  $t_0$ . Thus  $\lambda_0^*$  is the equilibrium field the medium would relax toward if the rupture maintained the specific form it had at the time  $t_0$ .

The basic integral representations in (5) and (6) can be evaluated in a relatively straightforward fashion for the case in which the material is uniformly prestressed in shear and when the basic failure has a spherical shape. Thus, for either instantaneous spherical shatter zone growth or for rupture growth at a rate less than the shear velocity, we can obtain closed-form solutions (see Archanbeau, 1968 and 1971). Further, we can allow the spherical zone to grow and to translate in time within the stressed medium, thereby simulating a propagating failure zone which heals itself, i.e., locks up a short time after the initiation of the failure. Thus we can calculate the field from a transient type of failure which sweeps through a

A-11

large region (see for details Archanbeau and Minster, 1971). All these solutions have the same analytic form; regarded as multi-pole fields in the frequency domain they are given by:

$$\chi_a^{(1)}(\underline{r}, \omega) = \sum_{l=2}^{\infty} h_l^{(2)}(k_a r) \sum_{m=0}^l [\Lambda_{lm}^a(\omega) \cos m\theta + B_{lm}^a(\omega) \sin m\theta] P_l^m(\cos \theta)$$

with

$$\Lambda_{lm}^a(\omega) = (-1)^l \frac{(l-m)!}{(l-2)!(2-m)!} G_l^a(\omega) \begin{bmatrix} 3\sigma_{23}^{(0)} & \sigma_{12}^{(0)} & \sigma_{23}^{(0)}/2 \\ -3\sigma_{13}^{(0)} & 0 & \sigma_{13}^{(0)}/2 \\ 0 & -\sigma_{12}^{(0)} & -\sigma_{12}^{(0)} \\ 0 & \sigma_{13}^{(0)} & 0 \end{bmatrix}$$

$$B_{lm}^a(\omega) = (-1)^l \frac{(l-m)!}{(l-2)!(2-m)!} H_l^a(\omega) \begin{bmatrix} 0 & 0 & -\sigma_{13}^{(0)}/2 \\ 0 & -\sigma_{12}^{(0)} & -\sigma_{23}^{(0)}/2 \\ 0 & \sigma_{13}^{(0)} & 0 \\ 0 & \sigma_{23}^{(0)} & \sigma_{12}^{(0)}/2 \end{bmatrix}$$

A-17

(see Archambeau, 1968 and 1971). The quantities  $\sigma_{ij}^{(0)}$  are the constant components of the pure shear prestress field we assume, and the matrices are indexed on  $\alpha = 1, 2, 3, 4$ , and  $m = 0, 1, 2$ . The prestress matrices and the functions  $G_{\ell}^{\alpha}$  and  $H_{\ell}^{\alpha}$  determine the nature of the multipole coefficients  $A_{\ell m}^{\alpha}$  and  $B_{\ell m}^{\alpha}$ . These functions are dependent on the type of rupture involved, and in general are rather complicated series of hypergeometric functions (derived in detail by Archambeau, 1968 and 1971, and Archambeau and Minster, 1971).